On the *independent irritability* of goldfish eggs and embryos – a living communication on the rhythmic yolk contractions in goldfish

Paul Gerald Layague Sanchez[1] ✉, **Chen-Yi Wang 王貞懿** [1], **Ing-Jia Li 李穎佳**[1], **and Kinya G. Ota 太田欽也**[1]

[1]Laboratory of Aquatic Zoology, Yilan Marine Research Station, Institute of Cellular and Organismic Biology, Academia Sinica, Taiwan

Rhythms play an important role in the precise spatiotemporal regulation of biological processes during development and patterning of embryos. We here investigate the rhythmic contractions of the yolk during early development of the goldfish *Carassius auratus*. We quantify these contractions and record robust and persistent rhythmic yolk movements that are not seen in closely-related species (carp and zebrafish). We report that yolk contractions are an intrinsic emergent property of the egg, i.e. goldfish eggs are independently irritable / excitable. These contractions do not require sperm entry / fertilization nor cell division, and they notably emerge at a precise time — suggesting that goldfish eggs are able to measure elapsed time from what we infer to be egg activation. As the yolk itself is known to confer critical cues for early dorsoventral (DV) patterning of teleost embryos, we hypothesize that its contractions in goldfish may influence the patterning process of this species. Indeed, we find that embryos in conditions that result in ventralized phenotypes (i.e. goldfish embryos acutely treated with microtubule-depolymerizing drug nocodazole and embryos of the twin-tail goldfish strain *Oranda*) display altered yolk contraction dynamics (i.e. faster and/or stronger contractions). We aim to uncover whether the yolk contractions happening during early development of domesticated goldfish are the licensing process which explain the variety of novel DV patterning phenotypes naturally-observed in this species (e.g. twin-tail and dorsal-finless strains) and which are instead not found among closely-related species (e.g. carp) whose yolks do not contract.

This manuscript is here published as a living communication (as described in Gnaiger (2021)). The authors intend to share findings when they are available, encourage feedback and discussion, and invite knowledge exchange and collaboration.

goldfish | yolk | rhythmic contractions | dorsoventral patterning
Correspondence: ***pglsanchez@gmail.com***

Introduction

Proper embryonic development and patterning require precise spatiotemporal regulation so that cellular and biochemical events occur at the right place and at the right time. This coordination is highly dynamic and is often mediated by processes that themselves exhibit dynamic behaviors, such as oscillations and waves (Cartwright et al., 2009; Deneke and Di Talia, 2018; Di Talia and Vergassola, 2022; Goodwin and Cohen, 1969; Turing, 1952; Uriu, 2016). The establishment of the animal body plan is a concrete example of the importance of such spatiotemporal regulation (Bénazéraf and Pourquié, 2013; Cooke, 1988; Grimes and Burdine, 2017; Hibi et al., 2018; Meinhardt, 2006), as variation in this process and deviations from archetypal development are often lethal or pathological, as is the case of congenital scoliosis (Pourquié, 2011). At the same time, variations in archetypal processes of body plan establishment are e.g. at the origin of the variety of unique phenotypes of the many present-day strains of domesticated goldfish *Carassius auratus* (Abe et al., 2014; Ota and Abe, 2016). One central question in both developmental biology and animal evolution thus remains that of how changes in the spatiotemporal regulation of common developmental programmes can give rise to such a diversity of body forms from a single cell, the egg.

A huge body of research pioneered and inspired by Ernest Everett Just has revealed over the years the dynamic processes involved in- and resulting from- the activation, fertilization, and patterning of the egg (Byrnes and Newman, 2014). E. E. Just advocated for melding of physics and biology in the study of embryonic development (Just, 1939) at a time when this was not common practice, and described the egg as "*self-acting, self-regulating and self-realizing – an independently irritable system*", i.e. an excitable soft matter (Byrnes and Newman, 2014; Newman, 2009). For instance, the egg exhibits dynamic changes of its cytoskeleton (Just, 1919, 1939; Santella and Chun, 2022), and waves of dynamic calcium signaling during activation and fertilization (Sardet et al., 1998; Stricker, 1999). These dynamics are now known to have the capacity to carry spatiotemporal information that pre-determines later developmental events, e.g. the site of gastrulation in ascidians (Roegiers et al., 1995; Sardet et al., 2007), and are linked to emergent contractile behavior of the egg (Brownlee and Dale, 1990; Ishii and Tani, 2021; Kyozuka et al., 2008; Limatola et al., 2022) in both ascidian eggs (Brownlee and Dale, 1990; Ishii and Tani, 2021) and in mouse oocytes (Deguchi et al., 2000).

Unlike the egg contractions mentioned above, which are short-lived and occur just after egg activation and fertilization (Brownlee and Dale, 1990; Deguchi et al., 2000; Ishii and Tani, 2021), some eggs and embryos also display rhythmic contractions that last until much later stages of development. For example, cell-autonomous periodic cortical waves of contraction (PeCoWaCo), linked to the softening of the actomyosin cortex, are evident during the cleavage stages pre-

ceding compaction in mouse embryos (Maître et al., 2015; Özgüç et al., 2022). Perhaps more strikingly, in goldfish embryos rhythmic contractions of the yolk surface emerge from the 4-cell stage and persist for hours until the epiboly stage of development (Yamamoto, 1934). These yolk contractions are faster at higher temperatures (Yamamoto, 1934), with temperature constants that cluster with those of processes that are mainly oxidative (Crozier, 1924) and those of others that are primarily involved in growth and development (Crozier, 1926).

The yolk of fish embryos has been shown to be more than just a static nutritional resource. In fact, experiments in both zebrafish and goldfish have shown that the yolk carries determinants for the establishment of the fish body plan, thus playing an active role in development and patterning. Specifically, the yolk has been shown to confer dorsal specification cues to developing fish embryos (Mizuno et al., 1999, 1997; Ober and Schulte-Merker, 1999). According to the paradigm defined in zebrafish, shortly after egg activation and fertilization and prior to the first cleavage a parallel array of microtubules that forms at the vegetal side of the yolk is crucial for the proper asymmetric transport of maternal dorsalizing determinants to the developing embryo's prospective dorsal organizer (Jesuthasan and Strähle, 1997; Tran et al., 2012). An analogous supply and asymmetrical partitioning of maternal axial determinants has been equally inferred in goldfish (Mizuno et al., 1997).

Interestingly, a wide variety of viable DV patterning phenotypes has been observed in fish. This is the case of the wide variety of median-fin-related morphological phenotypes (i.e. median fin morphotypes) of domesticated goldfish strains, which have been shown to arise from altered DV patterning during embryonic development. While there is evidence for an active role of the acellular yolk in this process, most studies on the matter have focused on underlying genetic and molecular mechanisms. It is now known that twin-tail goldfish carry a mutation in one of their chordin genes (i.e. *chdS*), which results in a non-functional truncated ChdS protein (Abe et al., 2014). Loss of function of said chordin gene, which naturally inhibits ventralization of the body (Piccolo et al., 1996; Sasai et al., 1994), is sufficient to cause caudal fin bifurcation in wild-type goldfish (Abe et al., 2014; Lee et al., 2023), and this mutation has been also recently implicated in loss of dorsal fin in dorsal finless goldfish strains (Chen et al., 2022). The spatiotemporal dynamics of the contractile goldfish yolk remains understudied in goldfish development and evolution, in particular, and in cell-developmental biology, in general.

Here, we aim to investigate the dynamic, emergent behavior of the goldfish yolk, hoping to learn more about its origin, its maintenance, and its role. In this manuscript, we share findings from our work addressing the following questions:

- On origin and maintenance of yolk contractions: How do the rhythmic yolk contractions emerge? How are they maintained?
- On mechanism and function of yolk contractions: Do the rhythmic yolk contractions have a function? Do they permit the emergence of diverse median fin morphotypes (DV patterning phenotypes) in domesticated goldfish?

About this version

This is the initial version of this manuscript, which we here publish as a living communication (as described in Gnaiger (2021)). We intend to share findings when they are available, encourage feedback and discussion, and invite knowledge exchange and collaboration.

Results

Extraction of yolk contraction timeseries from timelapses of developing goldfish embryos. We imaged developing goldfish embryos under the stereomicroscope and observed rhythmic yolk contractions starting at the 4-cell stage and persisting until later stages (Supplementary Movie M1), as reported by Yamamoto (1934). To quantify these contractions, we segmented the yolk and determined its circularity, its perimeter, and its projected area over time. We compared these values with the mean pixel value of the embryo, circumscribed by its chorion, over time (Figure 1A, Supplementary Movie M2), reasoning that still-frames of an embryo at the same phase of the yolk contraction would be most similar, and hence would have similar mean pixel values (Figure 1 A1 and A3, A2 and A4, or A5 and A8). We indeed noted that the mean pixel value of the embryo is a proxy of the projected area of the yolk, and henceforth used mean pixel value in our quantification of the yolk contractions. To analyze the contractions (Figure 1B), we detrended the timeseries via sinc-filter detrending after specifying a cut-off period. We subjected the detrended timeseries to continuous wavelet transform using the Morlet wavelet as mother wavelet (Mönke et al., 2020) and then recovered the instantaneous period, amplitude, and phase.

Goldfish, unlike closely-related carp and zebrafish, exhibit persistent rhythmic yolk contractions during embryonic development. Having established a pipeline for the quantification and analysis of yolk contractions from timelapse images, we compared goldfish yolk dynamics with those of a closely-related species, carp, and of another cyprinifom, zebrafish (Figure 1C-F, Supplementary Movie M3). Persistent and periodic yolk contractions were evident in goldfish embryos, but not in carp nor in zebrafish (Figure 1D). These contractions had a stable period of 135±2 seconds (133–137 seconds), or ∼ 2.25 mins, from 01:45:00 to 02:34:50 hh:mm:ss post-fertilization (n = 2) and have high wavelet power (Figure 1E-F, Supplementary Figure F1) correlating well with considered wavelets and not with white noise (Mönke et al., 2020). In zebrafish and carp embryos, we instead only noted high-period (or low-frequency) rhythms at ∼ 12.5 mins, with period of 753±4 seconds (749–757 seconds) for carp (n = 2) and 759.5±28.5 seconds (733–820

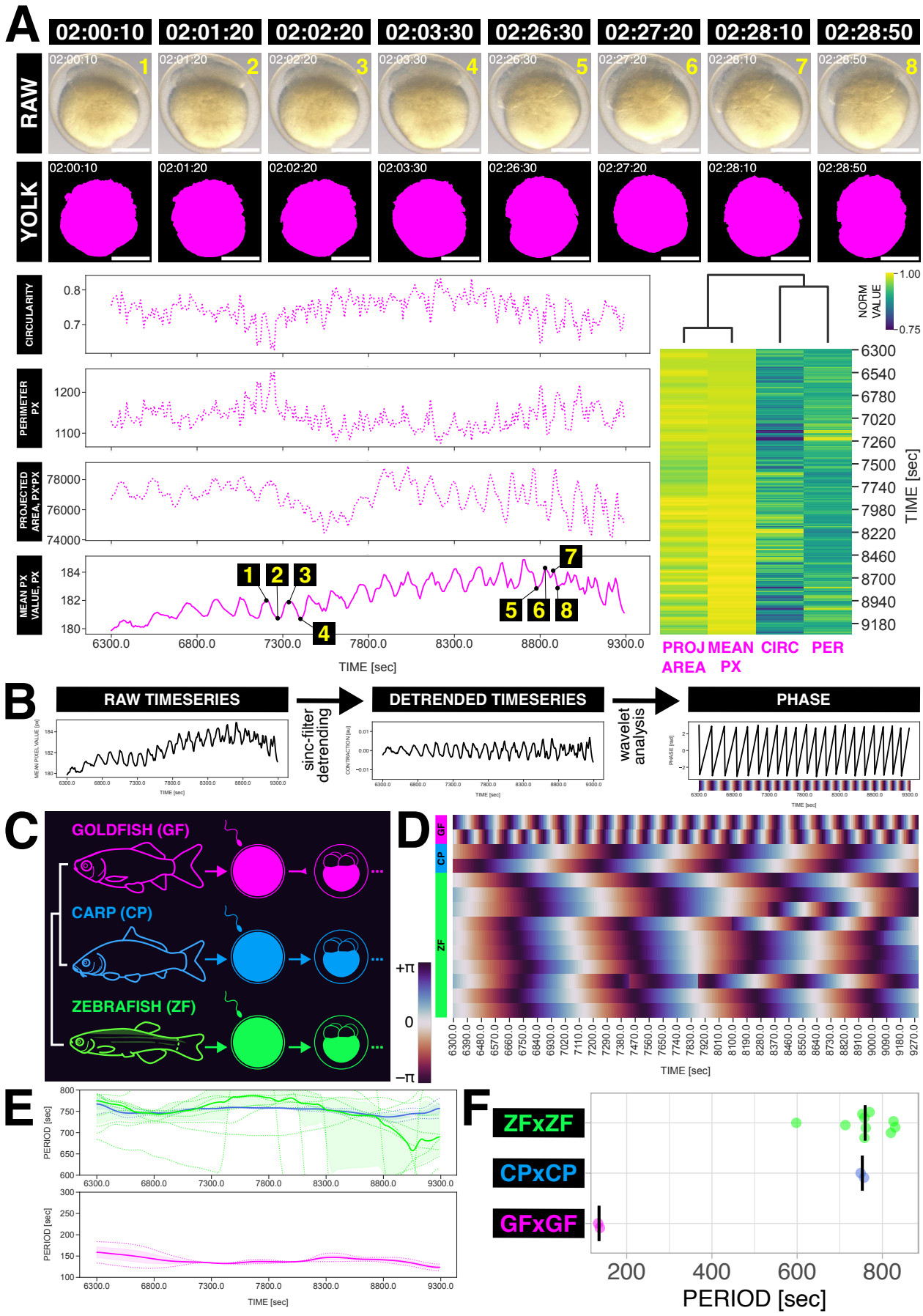

Fig. 1. Goldfish exhibit persistent yolk contractions during embryonic development, unlike closely-related carp and zebrafish. (**A**) Top panel: snapshots of a goldfish embryo and its segmented yolk (magenta) over time (hh:mm:ss post-fertilization). Scale bar = 500 μm. *Continued on the following page ...*

Fig. 1. ... *continued from the previous page.* Bottom-left panel: circularity, perimeter and projected area of the yolk, and mean pixel value of the embryo over time. Numbers (1–8) mark corresponding timepoints of snapshots shown in the top panel. Bottom-right panel: clustering of the timeseries shown in the bottom-left panel. These timeseries are shown with the timelapse of the goldfish embryo and its segmented yolk in Supplementary Movie M2. (**B**) Schematic of pipeline to analyze yolk contractions: (1) Raw timeseries is extracted from the mean pixel value of an embryo over time. (2) This timeseries is subjected to sinc-filter detrending using a cut-off period. (3) The detrended timeseries is then subjected to continuous wavelet transform and the instantaneous period, amplitude, and phase (shown here) are recovered. Phase over time can be represented as a phase heatmap using a cyclic colormap (e.g. twilight_shifted where maroon ($+\pi = -\pi$) corresponds to the trough of the detrended timeseries). (**C**) Schematic of experiment comparing embryos of goldfish (GF, magenta) with those of closely-related carp (CP, blue) and of another cypriniform zebrafish (ZF, green). (**D**) Phase heatmaps of detrended timeseries (via sinc-filter detrending, cut-off period = 850 seconds) of goldfish (n = 2), carp (n = 2), and zebrafish (n = 10) embryos at 6300–9290 seconds (or 01:45:00–02:34:50 hh:mm:ss) post-fertilization. Maroon ($+\pi = -\pi$) corresponds to the trough of the detrended timeseries. Corresponding detrended timeseries are shown in Supplementary Figure F1A. (**E**) Temporal evolution of period at 6300–9290 seconds (or 01:45:00–02:34:50 hh:mm:ss) post-fertilization, obtained from wavelet analysis. The period evolution for each sample and the median of the periods are represented as a color-coded dashed line and a color-coded solid line, respectively. The color-coded shaded area corresponds to the interquartile range. A similar plot is shown with the corresponding temporal evolution of wavelet power in Supplementary Figure F1B-C. (**F**) Average period of fish embryos at 6300–9290 seconds (or 01:45:00–02:34:50 hh:mm:ss) post-fertilization. Samples are represented as color-coded dots, while the median is denoted as a solid black line. Timelapse of some of the fish embryos are shown in Supplementary Movie M3.

seconds) for zebrafish (n = 10). We are not certain what these slow rhythms in carp and zebrafish embryos are, but they could be related to the ongoing embryonic cell divisions, which take $\sim$ 25 mins in carp (personal observations) and $\sim$ 15 mins in zebrafish (Kane and Kimmel, 1993). Nonetheless, such slow rhythms are clearly not the same as the persistent yolk contractions seen in goldfish.

The rhythmic contraction of the yolk is a trait that is maternal in origin. We next compared embryos of goldfish, carp, and their hybrids (Figure 2). Specifically, we generated reciprocal goldfish-carp hybrids by artificial fertilization (Tsai et al., 2013) (Figure 2A): (a) in one type of hybrids the egg was derived from goldfish and the sperm from carp, while (b) in the other type of hybrids the egg was derived from carp and the sperm from goldfish. We observed that yolk contractions were only detectable in embryos where the egg had been derived from goldfish (Figure 2B-C, Supplementary Movie M4). We conclude that the contractions of the yolk are of maternal origin, i.e. whether or not yolk contractions emerge in fish embryos depends on the egg.

The rhythmic contraction of the goldfish yolk is independent from fertilization or cell division, and emerge at a precise time. After noting that goldfish yolk contractions are of maternal origin, we asked whether fertilization of the egg is required to trigger this phenomenon. To address this question, we compared fertilized and unfertilized goldfish eggs (Figure 3A). Remarkably, unfertilized goldfish eggs not only showed rhythmic contractions; these also emerge at around the same time as they do in fertilized eggs, which start at $\sim$ 4-cell stage (Figure 3B, Supplementary Movie M5). Considering there is no real "4-cell" stage in unfertilized samples, as they fail to undergo cell divisions (Supplementary Movie M5), these results hint to an intrinsic timing mechanism to the beginning of yolk contractions relative to a certain reference "time 0" that could be egg activation, which in turn is triggered by contact with water (Lee et al., 1999; Yamamoto, 1954). Regardless, contractions of the yolk in unfertilized eggs persist for a long time until the cell eventually dies (Figure 3C-D, Supplementary Movie M5). Notably, unfertilized samples tend to have faster contractions than fertilized ones (Figure 3E). These data reveal that the contractions of the yolk do not require sperm entry / fertilization, and that they are are also not due to cell division, further supporting the idea that the goldfish egg is an independently irritable system, i.e. it is excitable (Newman, 2009). Upon passing a threshold, possibly initiated at egg activation, goldfish eggs are able to exhibit emergent contractile dynamics that persist for a long time.

The rhythmic contraction of the goldfish yolk does not depend on microtubule polymerization prior to first cleavage, and is not sufficient for proper DV patterning. The formation of parallel array of microtubules at the vegetal yolk immediately after egg activation and fertilization, prior to the first cleavage, is known to be crucial to the proper DV patterning of fish embryos (Jesuthasan and Strähle, 1997; Tran et al., 2012). To investigate if goldfish yolk contractions are linked to this process, we treated goldfish embryos with nocodazole, a microtubule depolymeryzing drug (Hoebeke et al., 1976). More precisely, at $\sim$ 10 mins post-fertilization (mpf), we incubated goldfish embryos in 0.1 μg/mL nocodazole for $\sim$ 4 mins, as previously done in zebrafish (Jesuthasan and Strähle, 1997). Yolk contractions persisted even after acute drug treatment (Figure 4A, Supplementary Movie M6). Incidentally, we also noted persistent contractions in yolk that pinched off from a dying treated embryo (n = 4, Supplementary Figure F2, Supplementary Movie M6 06:00:00 to 06:40:00 hh:mm:ss post-fertilization, Supplementary Movie M7). To verify the effectiveness of our drug treatment, we screened embryonic phenotypes at 1-day post-fertilization (dpf) (Figure 4B-C). As reported in zebrafish (Jesuthasan and Strähle, 1997), acute treatment of goldfish embryos with nocodazole prior to first cleavage resulted in axis patterning defects and mostly ventralized phenotypes (Figure 4C). We have not verified the presence of a parallel array of microtubules in the vegetal yolk of goldfish, as described in zebrafish. Nonetheless, these results indicate that the contractions of the goldfish yolk do not rely on a similar microtubule assembly during early development. More interestingly to our investigation, these experiments reveal that rhythmic yolk contractions *per se* do not ensure fidelity of axis patterning.

Faster and/or stronger yolk contractions correlate with conditions resulting in ventralized phenotypes. Considering the results of the previous experiments, we thought that perhaps what matters for proper DV patterning is not the presence or the absence of the yolk contractions, but rather the dynamics of these contractions. Indeed, we recorded

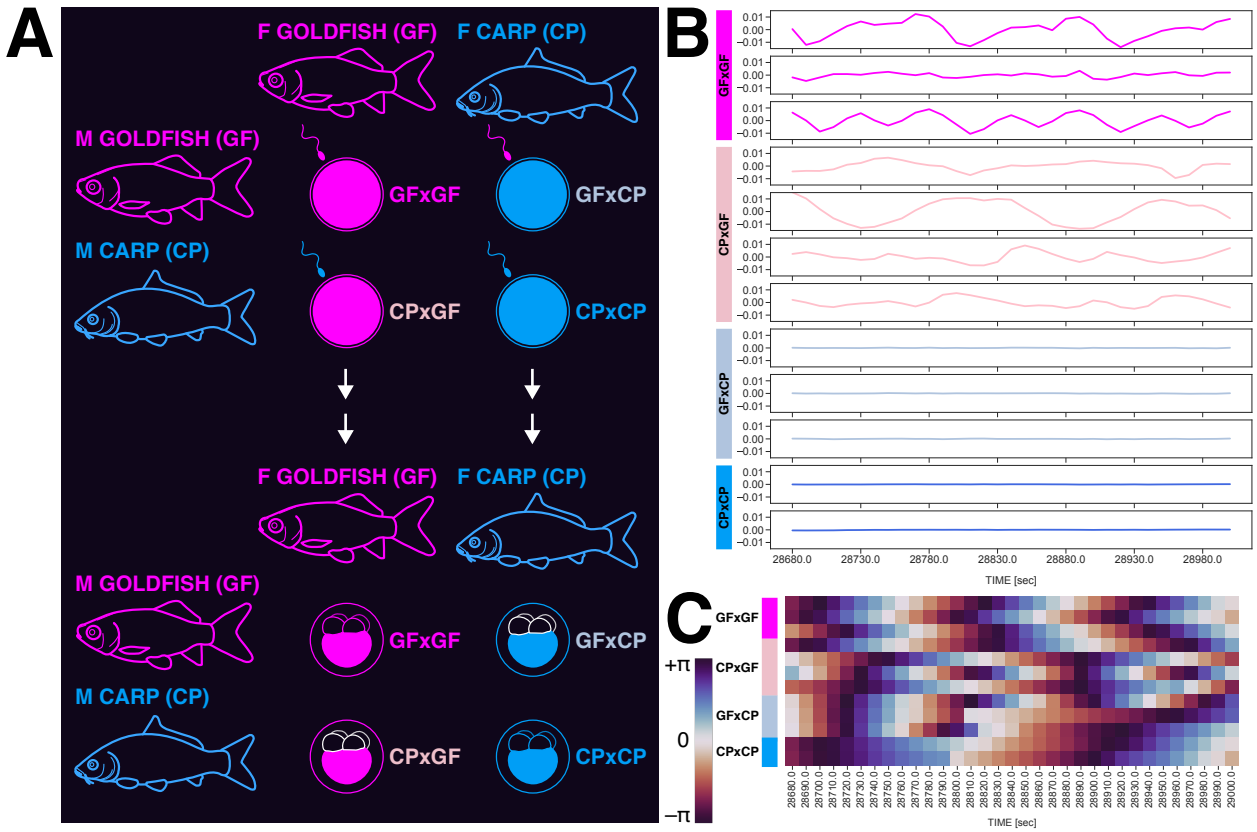

Fig. 2. Embryos that derive their egg from goldfish exhibit rhythmic yolk contractions. (**A**) Schematic of experiment comparing embryos of goldfish (GFxGF, magenta, n = 3), of carp (CPxCP, blue, n = 2), and of their reciprocal hybrids: CPxGF (light pink, n = 4) that is from carp sperm and goldfish egg, and GFxCP (light blue, n = 3) that is from goldfish sperm and carp egg. (**B**) Detrended timeseries (via sinc-filter detrending, cut-off period = 850 seconds) of fish embryos at 28680–29000 seconds (or 07:58:00–08:03:20 hh:mm:ss) post-fertilization. (**C**) Phase heatmaps of detrended timeseries of fish embryos at 28680–29000 seconds (or 07:58:00–08:03:20 hh:mm:ss) post-fertilization. Maroon ($+\pi = -\pi$) corresponds to the trough of the detrended timeseries. Timelapse of some of the fish embryos are shown in Supplementary Movie M4.

differences in the dynamics of yolk contractions when comparing nocodazole-treated embryos with controls (Figure 4D, Supplementary Movie M8). While both conditions show persistent yolk contractions, the contractions in embryos treated with nocodazole (n = 5), which results in ventralized embryos at 1dpf (Figure 4C), are faster (i.e. they have lower period of 150±2 seconds (133–152 seconds), Figure 4E) and stronger (i.e. they have higher amplitude of 1.46±0.26 a.u. (1.05–1.76 a.u.), Figure 4F) than their control counterparts (with period of 164±4 seconds (160–168 seconds) and amplitude of 0.73±0.17 a.u. (0.55–0.90 a.u.), n = 2).

We also compared wild-type goldfish with twin-tail goldfish *Oranda*, which is naturally more ventralized (Abe et al., 2014). While the amplitude of the contractions are comparable (i.e. the 95% confidence interval of the medians overlap) between the two strains (0.94±0.24 a.u. (0.7–1.18 a.u., n = 2) for wild-type and 0.76±0.18 a.u. (0.49–0.94 a.u., n = 5) for twin-tail), yolk contractions in twin-tail embryos are faster than in wild-type (Figure 5, Supplementary Movie M9) with periods of 118±1 seconds (116–125 seconds, n = 5) and 137 seconds (n = 2), respectively.

Thus, in both aforementioned contexts, faster and/or stronger yolk contractions correlate with conditions that result in ventralized phenotypes.

Discussion and open questions

The egg exhibits a range of dynamic behaviors during development and patterning such as cytoskeletal reorganisation, calcium signaling oscillations, waves, and contractile behavior (Brownlee and Dale, 1990; Deguchi et al., 2000; Ishii and Tani, 2021; Just, 1919, 1939; Kyozuka et al., 2008; Limatola et al., 2022; Santella and Chun, 2022; Sardet et al., 1998; Stricker, 1999) most evident immediately after egg activation and fertilization. Remarkably, in goldfish eggs and embryos (but not in those of closely-related carp and zebrafish) rhythmic contractions of the yolk emerge after some time elapsed from egg activation and fertilization and persist until gastrulation. These contractions are maternal and do not require sperm entry / fertilization nor cell division.

Egg activation does not require sperm and will be initiated when goldfish eggs contact water (Lee et al., 1999; Yamamoto, 1954), thus possibly functioning as a trigger and "time 0" reference for the emergence of yolk contractions even in unfertilized samples. We currently do not know why yolk contractions do not begin immediately after egg activation but instead become apparent only at a precise time (i.e. the 4-cell stage of fertilized eggs). This could perhaps be related to the timing of the 4-cell stage as a milestone in DV axis specification. For instance, maternal *sqt* RNA (*squint/nodal-related 1*), which is involved in DV pat-

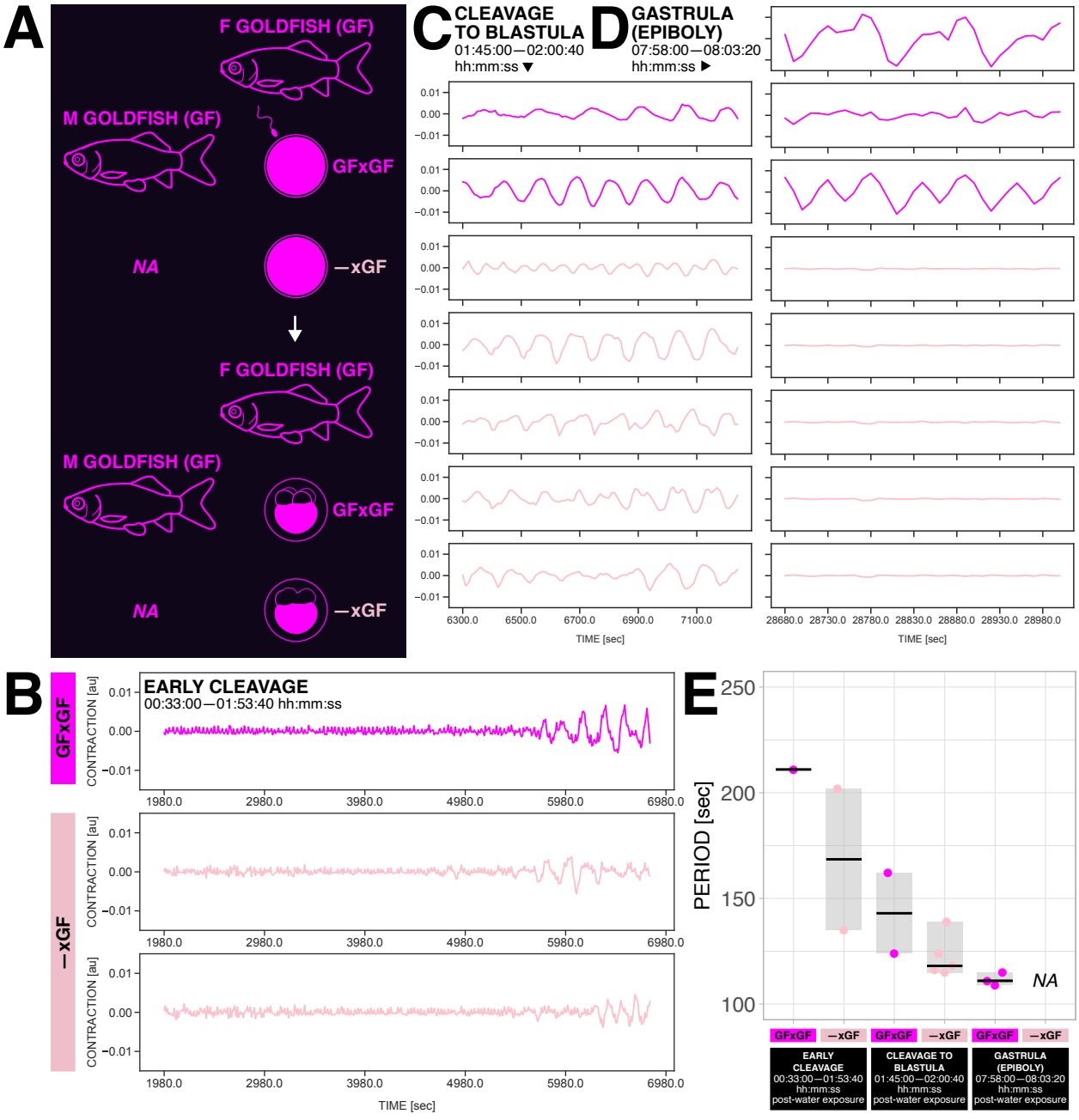

Fig. 3. The rhythmic contractions of the goldfish yolk do not require fertilization and emerge at a precise time. (**A**) Schematic of experiment comparing fertilized (GFxGF, magenta) and unfertilized (–xGF, light pink) goldfish eggs. (**B**) Detrended timeseries (via sinc-filter detrending, cut-off period = 250 seconds) of fertilized (n = 1) and unfertilized (n = 2) goldfish eggs at 1980–6820 seconds (or 00:33:00–01:53:40 hh:mm:ss) post-exposure of egg (and sperm, for fertilized sample) to water. Label for the time period is based on developmental staging of the fertilized sample. (**C**) Detrended timeseries (via sinc-filter detrending, cut-off period = 250 seconds) of fertilized (n = 5) and unfertilized (n = 5) goldfish eggs at 6300–7240 seconds (or 01:45:00–02:00:40 hh:mm:ss) post-exposure of egg (and sperm, for fertilized sample) to water. Label for the time period is based on developmental staging of fertilized samples. The fertilized samples are the same as the goldfish samples in Figure 1. (**D**) Detrended timeseries (via sinc-filter detrending, cut-off period = 250 seconds) of fertilized (n = 3) and unfertilized (n = 5) goldfish eggs at 28680–29000 seconds (or 07:58:00–08:03:20 hh:mm:ss) post-exposure of egg (and sperm, for fertilized sample) to water. Label for the time period is based on developmental staging of fertilized samples. The fertilized samples are the same as the goldfish (GFxGF) samples in Figure 2. (**E**) Average period of fertilized and unfertilized goldfish eggs at different time periods. Labels for each time period are based on developmental staging of fertilized samples (e.g. early cleavage stage at 00:33:00–01:53:40 hh:mm:ss post-exposure of egg (and sperm, for fertilized sample) to water). Samples are represented as color-coded dots, while the median is denoted as a solid black line. The shaded area marks the range. Average period of unfertilized eggs at last time period was not determined because all (n = 5/5) were dead. Timelapse of some of the samples are shown in Supplementary Movie M5.

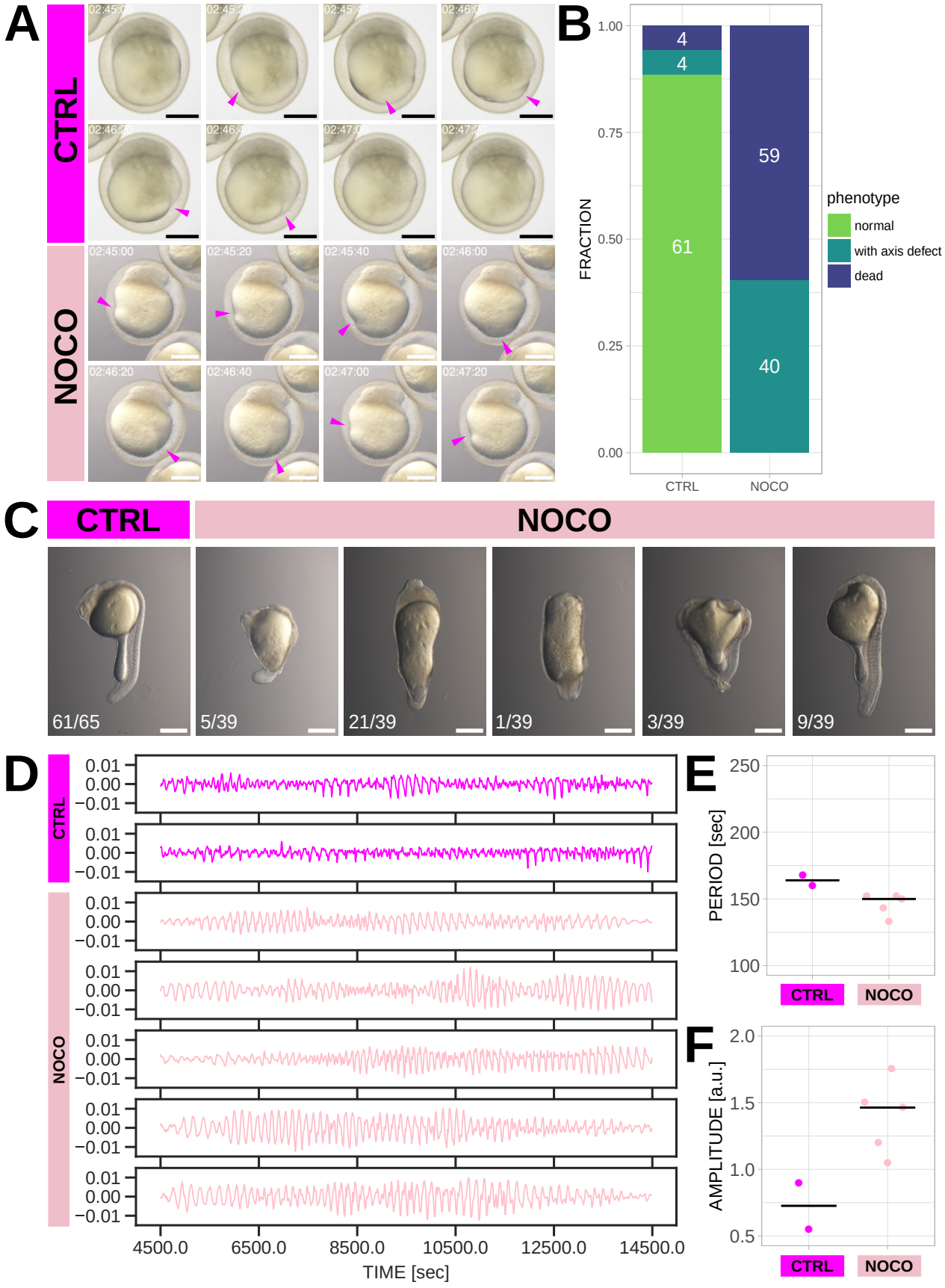

Fig. 4. The rhythmic contractions of the yolk persist in goldfish embryos acutely treated with a microtubule-depolymerizing drug prior to first cleavage but exhibit different dynamics than those in controls. (A) Snapshots of goldfish embryos at different timepoints indicated as hh:mm:ss post-fertilization (02:45:00–02:47:20 hh:mm:ss post-fertilization). Embryos were treated with either 0.1 μg/mL nocodazole (a microtubule-depolymerizing drug, NOCO, light pink) or DMSO (as control, CTRL, magenta) for $\sim$ 4 mins at $\sim$ 10 mins post-fertilization. Magenta arrowheads mark deformations of the yolk. Scale bar = 500 μm. Timelapse of these embryos are shown in Supplementary Movie M6. (**B**) Phenotypes of treated embryos (n = 99) and their respective controls (n = 69) at 1-day post-fertilization. *Continued on the following page ...*

Fig. 4. *... continued from the previous page.* (**C**) Representative images of surviving control and treated embryos at 1-day post fertilization. Scale bar = 500 μm. (**D**) Detrended timeseries (via sinc-filter detrending, cut-off period = 250 seconds) of yolk contractions in control (n = 2) and in treated (n = 5) goldfish embryos at 4500–14490 seconds (or 01:15:00–04:01:30 hh:mm:ss) post-fertilization. Timelapse of example embryos and their timeseries are shown in Supplementary Movie M8. (**E**) Average period of yolk contractions in control and treated goldfish embryos at 4500–14490 seconds (or 01:15:00–04:01:30 hh:mm:ss) post-fertilization. Samples are represented as color-coded dots, while the median is denoted as a solid black line. (**F**) Amplitude (at maximum wavelet power) of yolk contractions in control and treated goldfish embryos at 4500–14490 seconds (or 01:15:00–04:01:30 hh:mm:ss) post-fertilization. Samples are represented as color-coded dots, while the median is denoted as a solid black line.

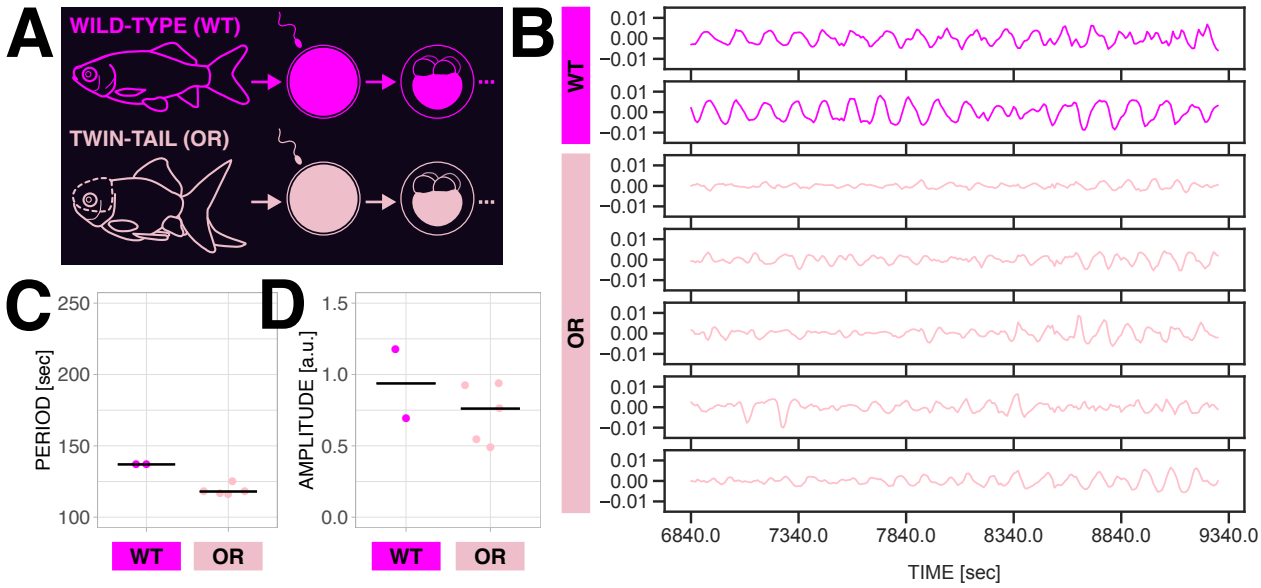

Fig. 5. Embryos of *Oranda*, a twin-tail goldfish strain, exhibit faster rhythmic yolk contractions than wild-type. (**A**) Schematic of experiment comparing yolk contractions in wild-type goldfish embryos (WT, magenta) and in twin-tail goldfish embryos (OR for *Oranda*, light pink). (**B**) Detrended timeseries (via sinc-filter detrending, cut-off period = 250 seconds) of yolk contractions in wild-type (n = 2) and in twin-tail (n = 5) goldfish embryos at 6840–9290 seconds (or 01:54:00–02:34:50 hh:mm:ss) post-fertilization. Timelapse of example embryos and their timeseries are shown in Supplementary Movie M9. The wild-type samples are the same as the goldfish samples in Figure 1 and the fertilized (GFxGF, magenta) samples in Figure 3C. (**C**) Average period of yolk contractions in wild-type and twin-tail goldfish embryos at 6840–9290 seconds (or 01:54:00–02:34:50 hh:mm:ss) post-fertilization. Samples are represented as color-coded dots, while the median is denoted as a solid black line. (**D**) Amplitude (at maximum wavelet power) of yolk contractions in wild-type and twin-tail goldfish embryos at 6840–9290 seconds (or 01:54:00–02:34:50 hh:mm:ss) post-fertilization. Samples are represented as color-coded dots, while the median is denoted as a solid black line.

terning, is distributed evenly in the egg but is transported to the animal pole via microtubules upon egg activation, even in the absence of sperm (Gore and Sampath, 2002). In fertilized eggs, it eventually becomes asymmetrically localized in 4-cell zebrafish embryos (Gore et al., 2005). Additionally, removal of the vegetal yolk after the 4-cell stage via surgical bisection along the equator of fish embryos does not result in severe ventralized phenotypes in goldfish (as is instead the case when the vegetal yolk cell is removed at the 2-cell stage Mizuno et al. (1997)), suggesting that a sufficient amount of the maternal dorsal determinants have been transported to the prospective dorsal organizer only by the 4-cell stage. Whether or not this timing is linked to the appearance of rhythmic yolk contractions is still unclear. Do the yolk contractions need the entire time from egg activation to organize their machinery (provided there is any)? Or do they already have the material/physical/chemical conditions for their execution early on, but "wait" until time equivalent to the 4-cell stage (e.g. until triggering of an activator and/or decay of an inhibitor)?

We hypothesize that the yolk contractions in goldfish are maintained by the cortical actomyosin network and/or calcium signaling. Both of these factors correlate spatiotemporally with contractile behavior in the ascidian egg after egg activation and fertilization (Brownlee and Dale, 1990; Ishii and Tani, 2021). Waves of calcium signaling are also involved in the deformation of mouse oocytes (Deguchi et al., 2000) and in the rhythmic contraction of the blastoderm in medaka embryos (Simon and Cooper, 1995). Softening of the cortical actomyosin network has also been recently implicated in the periodic cortical waves of contraction of mouse embryos prior to compaction (Özgüç et al., 2022). That the contractions persist in isolated yolk, e.g. in yolk pinched off from a dying embryo (Supplementary Figure F2, Supplementary Movie M6 06:00:00 to 06:40:00 hh:mm:ss post-fertilization, Supplementary Movie M7) and in vegetal yolk separated from the rest of the embryo as described by Mizuno et al. (1997), implies that the yolk itself is sufficient to exhibit said dynamic behavior (or that the yolk contractions do not rely on the embryo proper). Current knowledge on the link between cortical actomyosin, calcium signaling, and contractile behavior mainly focus on these phenomena in cells. It is thus curious to further investigate if these three similarly act in concert in an acellular biological system like the yolk. Indeed, it has been shown that an actomyosin network is sufficient to cause contractions in minimal synthetic models of cells. By tuning the ratio between actin and myosin, contractions can be induced in cortical actomyosin network reconstituted on a coverslip, in emulsion, or in lipid vesicles (Litschel et al., 2021; Miyazaki et al., 2015; Tsai et al., 2011).

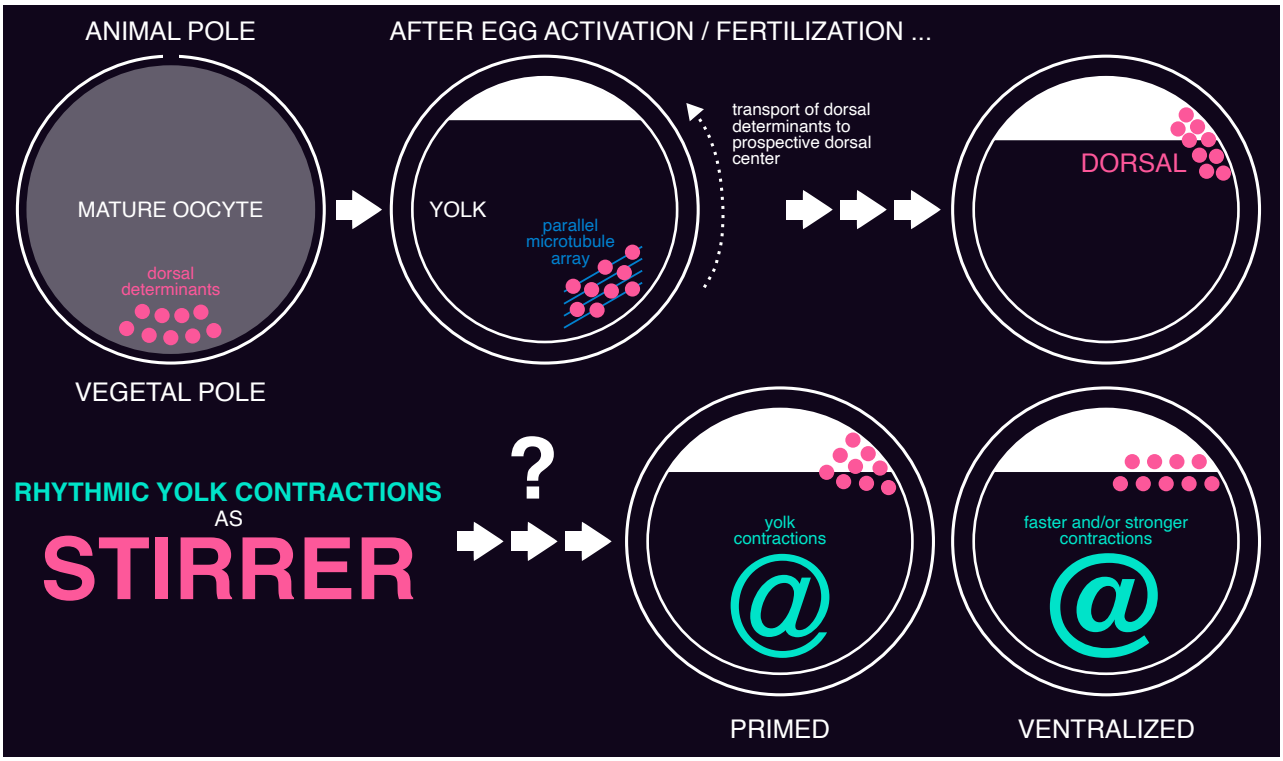

Fig. 6. The rhythmic yolk contractions in goldfish embryos could serve as a "stirrer" of dorsal determinants during DV patterning. After egg activation / fertilization, dorsal determinants deposited at the vegetal pole of mature fish oocytes are directed at an angle via a parallel microtubule array that forms at the vegetal side of the egg prior to the first cleavage (Jesuthasan and Strähle, 1997; Mizuno et al., 1999, 1997; Ober and Schulte-Merker, 1999; Tran et al., 2012). These determinants are then transported towards the animal pole, at the prospective dorsal center (Ge et al., 2014; Jesuthasan and Strähle, 1997; Tran et al., 2012). In the presence of rhythmic yolk contractions, as in goldfish embryos, the transport of these dorsal determinants from the vegetal pole to their target site are likely disturbed. If yolk contractions serve as a "stirrer", as previously suggested by Yamamoto (1934), then they could be spreading the determinants to a broader area, which would result in dilution at the prospective dorsal region and could permit the emergence of more ventralized phenotypes. Scheme on top row is adapted and modified from Ge et al. (2014); Hibi et al. (2002, 2018); Langdon and Mullins (2011); Nojima et al. (2010).

Contraction of the cortical actomyosin network in lipid vesicles could even result in surface deformations (Litschel et al., 2021). These deformations are however not periodic, suggesting that additional factors are likely involved in periodic contractions like those of the goldfish yolk. Indeed, linking actomyosin to calcium signaling in a theoretical model captures periodic deformations of non-adhering fibroblasts (Salbreux et al., 2007).

In terms of the function of the goldfish yolk contractions, we documented that conditions resulting in ventralized phenotypes correlate with faster and/or stronger contractions. Could yolk contraction dynamics (e.g. period and/or amplitude) then confer patterning cues to the developing fish embryo? Considering that the yolk carries material crucial for embryonic patterning, could yolk contractions serve as a "stirrer" as already suggested by Yamamoto (1934)? If the contractions serve as a stirrer, then they could be spreading maternally-derived dorsal determinants resulting in their dilution at the prospective dorsal organizer. This could be lowering the density of dorsalizing molecules available to counteract specification of ventral fates, e.g. via maternal *radar/gdf6a* (Goutel et al., 2000; Rissi et al., 1995; Sidi et al., 2003), therefore priming embryos for ventralization. In this "stirrer" framework (Figure 6), faster and/or stronger yolk contractions lead to further dilution of dorsal determinants and are thus correlated with more ventralized phenotypes.

Interestingly, faster calcium transients have been recorded in *hecate/grip2a* zebrafish mutants, which are ventralized (Ge et al., 2014; Gingerich et al., 2005). To the opposite, slowing down calcium transients via pharmacological perturbation of Ca^{2+} release results in ectopic expression of the dorsal marker *chordin* in zebrafish (Gingerich et al., 2005; Westfall et al., 2003). In fact, the zebrafish dorsal organizer has been shown to be a calcium pacemaker at the gastrula stage (Chen et al., 2017; Gilland et al., 1999). If calcium signaling is involved in goldfish yolk contractions, could these contractions be acting as an early determinant or an early readout of DV patterning in these fish? In the presence of contractions, could there be actual spatial spreading of maternally-derived dorsal determinants at the prospective dorsal organizer? And/or are there altered temporal dynamics between said molecules and target cells? It would be curious to elucidate how this is orchestrated with cytoskeleton-dependent transport.

Strikingly, altered DV patterning is implicated in the variation of median fin morphotypes in goldfish, such as twin-tail (Abe et al., 2014) and dorsal-finless (Chen et al., 2022). We documented here that embryos of *Oranda*, a twin-tail goldfish strain, exhibit faster yolk contractions than wild-type goldfish embryos, correlating faster and/or stronger contractions to more ventralized phenotypes in alignment to our current framework. Periodic contractions of the yolk were doc-

umented in embryos of a few other fish, e.g. those of the Japanese icefish *Salangichthys microdon* (Yamamoto, 1938). However, when considering a closely-related species with the same ecological niche, we noted that carp does not show rhythmic yolk contractions as goldfish. Could wild-type goldfish therefore already be more ventralized than carp? Interestingly, while it is easy to induce bifurcated tail fin in wild-type goldfish (e.g. by injecting morpholinos targeting *chdS* in embryos), similar ventralized phenotypes could not be achieved with carp (Abe et al., 2014, 2016). Notably, when investigating reciprocal goldfish-carp hybrids, we noted that rhythmic yolk contractions are present in hybrids with egg derived from goldfish. The egg cytoplasm was previously determined to impact traits (e.g. vertebra number) in goldfish-carp hybrids (Sun et al., 2005). Could hybrids exhibiting rhythmic yolk contractions then be more sensitive to perturbations resulting in bifurcated tail fin? Are these embryos primed for ventralization? Could yolk contractions be permissive of the emergence of median fin morphotypes?

Future perspectives

Increasing sample numbers and comparisons between clutchmates will be important to further strengthen the findings presented here. Lengthening the timelapse imaging will also be necessary to better analyze the dynamics throughout development (e.g. if/how the period of the contractions changes in a sample over time). We here propose further experimental plans to address open questions mentioned in the current study, and aimed to further elucidate the origin, the maintenance, and the role of rhythmic yolk contractions in goldfish.

On investigating yolk contraction and its dynamics. Alternative ways to extract the timeseries could be considered, especially those able to describe the yolk contractions in 3D. Through these more complete approaches, and perhaps in tandem with particle image velocimetry (Özgüç et al., 2022; Pereyra et al., 2021), one could more clearly relate the propagation and number of the waves of contractions to the position of the prospective dorsal organizer. This will necessitate imaging the embryo at higher spatial (i.e. 3D) and temporal (contractions are at the 10^2 seconds range) resolutions, requiring more sophisticated imaging modalities, likely at the expense of throughput. Quantitative measurements of the deformability of the yolk and of other viscoelastic properties would also be informative and could be achieved through micropipette aspiration (Guevorkian and Maître, 2017). In collaboration with theoreticians, modeling and numerical experiments could be done, e.g. on linking dynamic phenomena to transfer of material from one part of a contracting/deformable sphere to another.

On investigating cytoskeleton and its dynamics. To elucidate the contribution of the cytoskeleton on the rhythmic yolk contractions, it would be insightful to image and to quantify yolk contraction dynamics in goldfish embryos treated with either latrunculin, which interferes with actin polymer assembly (Spector et al., 1983), or blebbistatin, which disrupts interactions of actin and myosin (Straight et al., 2003). Generation of transgenic goldfish expressing an actin reporter, e.g. fluorescent protein fused to actin-binding domain of utrophin (Burkel et al., 2007), would be advantageous to study actin dynamics during yolk contractions. While CRISPR-Cas has been done in goldfish (Lee et al., 2023; Yu et al., 2022), generation of the transgenic remains challenging due to the restricted spawning season of this fish. Alternatively, goldfish embryos could be injected with fluorescent reporters of actin, e.g. fluorescently labeled phalloidin as done by Kyozuka et al. (2008) in starfish oocytes or mRNA of LifeAct fused to a fluorescent protein as done by Foster et al. (2022) also in starfish oocytes, prior to timelapse imaging. Immunostaining (e.g. with β-tubulin antibody and labeled phalloidin) of fixed goldfish embryos could also be done to evaluate the organization of the cytoskeleton at different phases of the yolk contractions.

On investigating calcium signaling and its dynamics. To elucidate the contribution of calcium signaling on the rhythmic yolk contractions, it would be insightful to image and to quantify yolk contraction dynamics in goldfish embryos treated with either phorbol 12-myristate 13-acetate (PMA) or bisindolylmaleimide I (BIM), which have been shown to speed up and slow down Ca^{2+} oscillations, respectively (Halet et al., 2004). Generation of transgenic goldfish expressing reporter of calcium signaling, e.g. GCaMP6s (Chen et al., 2013), would be advantageous to study calcium signaling dynamics during yolk contractions. As an alternative to generating a transgenic reporter strain e.g. via CRISPR-Cas, goldfish embryos could be injected with fluorescent calcium indicators, e.g. Oregon green dextran (OGD) as done by Mohri and Kyozuka (2022) in starfish oocytes, prior to timelapse imaging.

On investigating early DV patterning in goldfish embryos in relation to their yolk contractions. To relate the contraction of the yolk to DV patterning, and resolve their role as determinants or readouts, markers of DV patterning (e.g. *goosecoid*, *chordin*, nuclear β-catenin) could be used as additional readouts in the experiments cited above. The distribution of maternal dorsal determinants (e.g. *wnt8a* RNA) could be monitored either via in-situ hybridization of fixed embryos at different cleavage stages or via imaging of fluorescently-labeled *wnt8a* injected into live embryos, as done by Tran et al. (2012) in zebrafish embryos. Systematic comparison of the dorsal organizer domain in contractile goldfish and non-contractile carp would also be informative. Injection of *chdS* morpholino into goldfish-carp hybrid embryos would resolve whether a bifurcated tail fin can be induced in carp (hybrids) provided rhythmic yolk contractions occur.

Methods

Fish strains. Wild-type and twin-tail goldfish were obtained from an aquarium supplier in Taiwan. Carp were obtained from local breeders or directly caught from the Erlong (二龍)

river system in Yilan, Taiwan. Zebrafish were obtained from the Taiwan Zebrafish Core Facility at Academia Sinica (TZCAS). All experiments were conducted according to guidelines and upon approval of the Institutional Animal Care and Use Committee (IACUC) of Academia Sinica (Protocol #19-11-1351 and Protocol #22-11-1922).

Artificial fertilization of goldfish and carp eggs. During spawning season (March to June), artificial fertilization was performed as described in Tsai et al. (2013). Briefly, on the night before artificial fertilization, mature goldfish were injected with Ovaprim (Syndel, US) to stimulate production and maturation of gametes: $\sim$ 0.5 mL Ovaprim per kg of female fish and $\sim$ 0.1 mL Ovaprim per kg of male fish. After 12-16 hours, sperm and egg were collected. To collect sperm, male fish were gently squeezed near the cloaca and sperm was collected into labeled syringe pre-filled with Modified Kurokawa's extender 2 solution. Sperm activity was assessed by diluting a drop of sperm with water on a coverslip and visualizing sperm motility under the microscope. After confirming sperm activity, sperm was kept at 4^{o}C until use. To collect mature eggs, female fish was squeezed near the cloaca, which had been pat-dried, and eggs were collected onto PTFE dish. Adult fish were anesthetized in MS-222 (Supelco, #A5040) before handling, and were immediately allowed to recover in fresh tap water afterwards.

Drops of sperm were mixed with the eggs and the mixture was transferred to labeled plastic dishes (pre-coated with "Cha-Li-Wang" green tea (茶裏王, Uni-President Corp., Taiwan) to ease detachment of embryos from dish) containing tap water. For experiments involving unfertilized eggs, eggs were immediately transferred to dish containing tap water, without addition of sperm. After around 5 mins, water was removed and the eggs were washed at least 5 times with tap water. Optionally, the eggs were bleached with 0.1% (v/v, 1 mL in 1 L) bleach (Magic Amah, Taiwan) for 5 mins and quickly neutralized with 0.05% (w/v, 0.5 g in 1 L) sodium thiosulfate prior to washing. Eggs and embryos were kept in tap water at room temperature ($\sim$24^{o}C).

Mating and embryo recovery of zebrafish. On the late afternoon before mating, mature male (1) and female (1-2) zebrafish were put in a mating tank and were separated by a physical barrier. At dawn, when the lights were turned on, the barrier was removed and fish were allowed to mate. Embryos were recovered $\sim$5-10 mins after egg release, washed with E3 medium, transferred to labeled plastic dish containing E3, and incubated at room temperature ($\sim$24^{o}C).

Drug treatment. Stock solution of nocodazole (2 mg/mL) was prepared by mixing 2 mg of nocodazole (Sigma-Aldrich, #M1404) with 1 mL of DMSO (J.T.Baker, #9224-01 0121 24). Working solutions were freshly prepared: 2 uL of 2 mg/mL nocodazole in 40 mL solution with tap water (final concentration = 0.1 μg/mL nocodazole), and 2 uL of DMSO in 40 mL solution with tap water (as control). As in Jesuthasan and Strähle (1997), at $\sim$ 10 mpf (after bleaching and neutralization), embryos were incubated in nocodazole (or DMSO) for $\sim$ 4 mins. After incubation, embryos were washed at least 5 times with tap water. Embryos were kept in tap water at room temperature ($\sim$24^{o}C). Some embryos were subjected to timelapse imaging for analysis of yolk contraction dynamics. The rest of the embryos were kept at 24^{o}C and their phenotypes were analyzed at 1 dpf.

Imaging. Embryos were kept on the plastic dish and imaged at room temperature ($\sim$24^{o}C) using either an Olympus SZX16 microscope equipped with a DP80 digital camera (Olympus) or an Olympus BX53 microscope equipped with a DP27 digital camera (Olympus). To minimize evaporation of water, plastic dishes containing the embryos were covered with plastic lid that has a hole just on the field of view. Timelapse images were taken using the Process Manager of cellSens Standard software (Olympus) with a temporal resolution of either 10 seconds or 1 min. Access to metadata of timelapse imaging is available in `DATA-ImagingTimeseries` at https://github.com/PGLSanchez/yolk-contractions.

Data analysis. To extract the timeseries of yolk perimeter, circularity, and projected area, segmentation was first done using Simple Interactive Object Extraction (SIOX) plugin (Friedland et al., 2006) in Fiji (Schindelin et al., 2012) [in Fiji: `Plugins > Segmentation > SIOX: Simple Interactive Object Extraction`]. Using one frame, multiple regions within the yolk were specified as foreground [in SIOX: `Foreground`] and segmented [in SIOX: `Segment`]. The segmentation information was then saved [in SIOX: `Save segmentator`]. This segmentation was then applied to the rest of the stack [in Fiji: `Plugins > Segmentation > Apply saved SIOX segmentator`]. A binary mask, corresponding to the yolk, was then created for each frame of the stack. The circularity, perimeter, and area of this mask over time was analyzed using a Fiji macro (.ijm) available at https://github.com/PGLSanchez/yolk-contractions, which iterates `Analyze > Measure` over all frames in a stack.

For most of the analyses, the timeseries of each sample was extracted using Fiji by specifying a circular ROI marking the chorion and plotting the z-axis profile [in Fiji: `Image > Stacks > Z Project`], which plots the mean pixel value over time. When comparing conditions, samples with same hh:mm:ss post-fertilization (or hh:mm:ss after exposure to water) were considered which unfortunately restricted the sample numbers. Access to raw timeseries is available in `DATA-ImagingTimeseries` at https://github.com/PGLSanchez/yolk-contractions.

Raw timeseries was detrended using sinc-filter detrending after specifying a cut-off period. The cut-off period was determined empirically, which was set to be 250 seconds for all analyses except when comparisons were done between goldfish, carp, and zebrafish. Then, a cut-off period of 850 seconds was used to account for high-period rhythms in carp and zebrafish. Detrended timeseries was

subjected to continuous wavelet transform (with the Morlet wavelet as mother wavelet) using a wavelet analysis workflow (Mönke et al., 2020), which is also implemented as a Python-based standalone software available at https://github.com/tensionhead/pyBOAT (pyBOAT 0.9.11). A ridge tracing maximum wavelet power for each timepoint was detected and the instantaneous period, phase, and amplitude were extracted from this ridge. A high power (power > 3) indicates strong correlation of the wavelet with the signal versus white noise. The Python code used in data analysis is available as a Jupyter notebook (.ipynb) at https://github.com/PGLSanchez/yolk-contractions. This code uses Matplotlib (Hunter, 2007), NumPy (Harris et al., 2020; Van Der Walt et al., 2011), pandas (McKinney, 2010), scikit-image (Van der Walt et al., 2014), SciPy (Virtanen et al., 2020), and seaborn (Waskom, 2021).

For comparing the timeseries of embryo mean pixel value with the timeseries of yolk circularity, yolk perimeter, and yolk projected area, clustering was done on normalized timeseries using `seaborn.clustermap`.

For plots specifying one period per sample, estimation of the Fourier spectrum was done after wavelet analysis using pyBOAT 0.9.11 [in pyBOAT 0.9.11: `Time Averaging > Estimate Fourier`] and the period with highest power was considered. For plots specifying one amplitude per sample, the amplitude at timepoint with highest wavelet power was considered. These plots were generated- and summary statistics were calculated using PlotsOfData (Postma and Goedhart, 2019), which is available as a Shiny app at https://huygens.science.uva.nl/PlotsOfData. Period and amplitude were expressed as median ± median absolute deviation (95% confidence interval of the median) when indicated in the text.

ACKNOWLEDGEMENTS

We thank (in alphabetical order) Hsiao-Chian Chen 陳筱茜, Tetsuya Hiraiwa 平岩徹也, Shu-Hua Lee 李淑華, Daniel Ríos Barrera, Stephan Q. Schneider, Stefano Davide Vianello, Jr-Kai Yu 游智凱, former and present members of the Laboratory of Aquatic Zoology at the Yilan Marine Research Station (Yilan MRS), and all members of the EcoEvoDevo Internal Group of the Institute of Cellular and Organismic Biology (ICOB), Academia Sinica for the in-depth discussions and feedback. We likewise thank (in alphabetical order) Chen-Hui Chen 陳振輝, Kuo-Chiang Hsia 夏國强, Athira Saju, Stephan Q. Schneider, and Grace Sonia for the sharing of reagents. We are grateful to Wei-Chen Chu 朱韋臣 of the Imaging Core Facility of ICOB and to all the administrative staff and aquaculture specialists of Yilan MRS. We are also thankful to Ricardo Henriques for kindly sharing the template that was used to format this manuscript, and we are grateful to Daniel Ríos Barrera and Stefano Davide Vianello for critical reading and editing. This work was supported by an Academia Sinica Career Development Award (CDA-103-L05), a Japan Society for the Promotion of Science Grant (JSPS KAKENHI Grant JP16K18546), and Taiwan National Science and Technology Council (formerly Ministry of Science and Technology) Grants (MOST Grant 109-2311-B-001-027-MY3 and NSTC Grant 112-2311-B-001-033).

AUTHOR ORCID

Paul Gerald Layague Sanchez https://orcid.org/0000-0001-6213-8927
Chen-Yi Wang 王貞懿 https://orcid.org/0000-0003-4342-5140
Ing-Jia Li 李穎佳 https://orcid.org/0000-0001-6407-5181
Kinya G. Ota 太田欽也 https://orcid.org/0000-0002-6306-6790

AUTHOR CONTRIBUTIONS

Conceptualization: Paul Gerald Layague Sanchez (P). **Data curation**: P. **Formal Analysis**: P. **Funding Acquisition**: Kinya G. Ota 太田欽也 (K). **Investigation**: P, K. **Methodology**: P, Chen-Yi Wang 王貞懿 (C), Ing-Jia Li 李穎佳 (I), K. **Project Administration**: P, K. **Resources**: C, I, K. **Software**: P. **Supervision**: P, K. **Validation**: P, C, I, K. **Visualization**: P. **Writing – Original Draft**: P. **Writing – Review & Editing**: P.

	P	C	I	K
Conceptualization	■			
Data curation	■			
Formal Analysis	■			
Funding Acquisition				■
Investigation	■			■
Methodology	■	■	■	■
Project Administration	■			■
Resources		■	■	■
Software	■			
Supervision	■			■
Validation	■	■	■	■
Visualization	■			
Writing - Original Draft	■			
Writing - Review and Editing	■			

COMPETING FINANCIAL INTERESTS

The authors declare no competing financial interests.

Bibliography

Abe, G., Lee, S.-H., Chang, M., Liu, S.-C., Tsai, H.-Y., and Ota, K. G. (2014). The origin of the bifurcated axial skeletal system in the twin-tail goldfish. *Nature communications*, 5(1):3360.

Abe, G., Lee, S.-H., Li, I.-J., Chang, C.-J., Tamura, K., and Ota, K. G. (2016). Open and closed evolutionary paths for drastic morphological changes, involving serial gene duplication, subfunctionalization and selection. *Scientific reports*, 6(1):26838.

Bénazéraf, B. and Pourquié, O. (2013). Formation and segmentation of the vertebrate body axis. *Annual review of cell and developmental biology*, 29:1–26.

Brownlee, C. and Dale, B. (1990). Temporal and spatial correlation of fertilization current, calcium waves and cytoplasmic contraction in eggs of ciona intestinalis. *Proceedings of the Royal Society of London. B. Biological Sciences*, 239(1296):321–328.

Burkel, B. M., Von Dassow, G., and Bement, W. M. (2007). Versatile fluorescent probes for actin filaments based on the actin-binding domain of utrophin. *Cell motility and the cytoskeleton*, 64(11):822–832.

Byrnes, W. M. and Newman, S. A. (2014). Ernest everett just: Egg and embryo as excitable systems. *Journal of Experimental Zoology Part B: Molecular and Developmental Evolution*, 322(4):191–201.

Cartwright, J. H., Piro, O., and Tuval, I. (2009). Fluid dynamics in developmental biology: moving fluids that shape ontogeny. *HFSP journal*, 3(2):77–93.

Chen, H.-C., Wang, C., Li, I.-J., Abe, G., and Ota, K. G. (2022). Pleiotropic functions of chordin gene causing drastic morphological changes in ornamental goldfish. *Scientific Reports*, 12(1):19961.

Chen, J., Xia, L., Bruchas, M. R., and Solnica-Krezel, L. (2017). Imaging early embryonic calcium activity with gcamp6s transgenic zebrafish. *Developmental biology*, 430(2):385–396.

Chen, T.-W., Wardill, T. J., Sun, Y., Pulver, S. R., Renninger, S. L., Baohan, A., Schreiter, E. R., Kerr, R. A., Orger, M. B., Jayaraman, V., et al. (2013). Ultrasensitive fluorescent proteins for imaging neuronal activity. *Nature*, 499(7458):295–300.

Cooke, J. (1988). The early embryo and the formation of body pattern. *American Scientist*, 76(1):35–41.

Crozier, W. J. (1924). On biological oxidations as function of temperature. *The Journal of General Physiology*, 7(2):189–216.

Crozier, W. J. (1926). On curves of growth, especially in relation to temperature. *The Journal of General Physiology*, 10(1):53–73.

Deguchi, R., Shirakawa, H., Oda, S., Mohri, T., and Miyazaki, S. (2000). Spatiotemporal analysis of ca2+ waves in relation to the sperm entry site and animal–vegetal axis during ca2+ oscillations in fertilized mouse eggs. *Developmental biology*, 218(2):299–313.

Deneke, V. E. and Di Talia, S. (2018). Chemical waves in cell and developmental biology. *Journal of Cell Biology*, 217(4):1193–1204.

Di Talia, S. and Vergassola, M. (2022). Waves in embryonic development. *Annual review of biophysics*, 51:327–353.

Foster, P. J., Fürthauer, S., and Fakhri, N. (2022). Active mechanics of sea star oocytes. *bioRxiv*, pages 2022–04.

Friedland, G., Jantz, K., Lenz, T., and Rojas, R. (2006). Extending the siox algorithm: alternative clustering methods, sub-pixel accurate object extraction from still images, and generic video segmentation.

Ge, X., Grotjahn, D., Welch, E., Lyman-Gingerich, J., Holguin, C., Dimitrova, E., Abrams, E. W., Gupta, T., Marlow, F. L., Yabe, T., et al. (2014). Hecate/grip2a acts to reorganize the cytoskeleton in the symmetry-breaking event of embryonic axis induction. *PLoS genetics*, 10(6):e1004422.

Gilland, E., Miller, A. L., Karplus, E., Baker, R., and Webb, S. E. (1999). Imaging of multicellular large-scale rhythmic calcium waves during zebrafish gastrulation. *Proceedings of the National Academy of Sciences*, 96(1):157–161.

Gingerich, J. L., Westfall, T. A., Slusarski, D. C., and Pelegri, F. (2005). Hecate, a zebrafish maternal effect gene, affects dorsal organizer induction and intracellular calcium transient frequency. *Developmental biology*, 286(2):427–439.

Gnaiger, E. (2021). Beyond counting papers–a mission and vision for scientific publication. *Bioenergetics Communications*, 2021:5–5.

Goodwin, B. C. and Cohen, M. H. (1969). A phase-shift model for the spatial and temporal organization of developing systems. *Journal of Theoretical Biology*, 25(1):49–107.

Gore, A. V., Maegawa, S., Cheong, A., Gilligan, P. C., Weinberg, E. S., and Sampath, K. (2005). The zebrafish dorsal axis is apparent at the four-cell stage. *Nature*, 438(7070):1030–1035.

Gore, A. V. and Sampath, K. (2002). Localization of transcripts of the zebrafish morphogen squint is dependent on egg activation and the microtubule cytoskeleton. *Mechanisms of development*, 112(1-2):153–156.

Goutel, C., Kishimoto, Y., Schulte-Merker, S., and Rosa, F. (2000). The ventralizing activity of radar, a maternally expressed bone morphogenetic protein, reveals complex bone morphogenetic protein interactions controlling dorso-ventral patterning in zebrafish. *Mechanisms of development*, 99(1-2):15–27.

Grimes, D. T. and Burdine, R. D. (2017). Left–right patterning: breaking symmetry to asymmetric morphogenesis. *Trends in Genetics*, 33(9):616–628.

Guevorkian, K. and Maître, J.-L. (2017). Micropipette aspiration: A unique tool for exploring cell and tissue mechanics in vivo. In *Methods in cell biology*, volume 139, pages 187–201. Elsevier.

Halet, G., Tunwell, R., Parkinson, S. J., and Carroll, J. (2004). Conventional pkcs regulate the temporal pattern of ca2+ oscillations at fertilization in mouse eggs. *The Journal of cell biology*, 164(7):1033–1044.

Harris, C. R., Millman, K. J., Van Der Walt, S. J., Gommers, R., Virtanen, P., Cournapeau, D., Wieser, E., Taylor, J., Berg, S., Smith, N. J., et al. (2020). Array programming with numpy. *Nature*, 585(7825):357–362.

Hibi, M., Hirano, T., and Dawid, I. B. (2002). Organizer formation and function. *Pattern Formation in Zebrafish*, pages 48–71.

Hibi, M., Takeuchi, M., Hashimoto, H., and Shimizu, T. (2018). Axis formation and its evolution in ray-finned fish. *Reproductive and Developmental Strategies: The Continuity of Life*, pages 709–742.

Hoebeke, J., Van Nijen, G., and De Brabander, M. (1976). Interaction of oncodazole (r 17934), a new anti-tumoral drug, with rat brain tubulin. *Biochemical and biophysical research communications*, 69(2):319–324.

Hunter, J. D. (2007). Matplotlib: A 2d graphics environment. *Computing in science & engineering*, 9(03):90–95.

Ishii, H. and Tani, T. (2021). Dynamic organization of cortical actin filaments during the ooplasmic segregation of ascidian ciona eggs. *Molecular Biology of the Cell*, 32(3):274–288.

Jesuthasan, S. and Strähle, U. (1997). Dynamic microtubules and specification of the zebrafish embryonic axis. *Current Biology*, 7(1):31–42.

Just, E. (1919). The fertilization reaction in echinarachnius parma: I. cortical response of the egg to insemination. *The Biological Bulletin*, 36(1):1–10.

Just, E. E. (1939). *The biology of the cell surface*. P. Blakiston's Son and Co., Inc., Philadelphia, USA.

Kane, D. A. and Kimmel, C. B. (1993). The zebrafish midblastula transition. *Development*, 119(2):447–456.

Kyozuka, K., Chun, J. T., Puppo, A., Gragnaniello, G., Garante, E., and Santella, L. (2008). Actin cytoskeleton modulates calcium signaling during maturation of starfish oocytes. *Developmental biology*, 320(2):426–435.

Langdon, Y. G. and Mullins, M. C. (2011). Maternal and zygotic control of zebrafish dorsoventral axial patterning. *Annual review of genetics*, 45:357–377.

Lee, K. W., Webb, S. E., and Miller, A. L. (1999). A wave of free cytosolic calcium traverses zebrafish eggs on activation. *Developmental biology*, 214(1):168–180.

Lee, S.-H., Wang, C. Y., Li, J., Abe, G., and Ota, K. (2023). Competition or contingency? using crispr/cas9-induced mutants to examine the potential origin of a unique mutant allele in twintail goldfish. *Research Square*.

Limatola, N., Chun, J. T., and Santella, L. (2022). Regulation of the actin cytoskeleton-linked ca2+ signaling by intracellular ph in fertilized eggs of sea urchin. *Cells*, 11(9):1496.

Litschel, T., Kelley, C. F., Holz, D., Adeli Koudehi, M., Vogel, S. K., Burbaum, L., Mizuno, N., Vavylonis, D., and Schwille, P. (2021). Reconstitution of contractile actomyosin rings in vesicles. *Nature communications*, 12(1):2254.

Maître, J.-L., Niwayama, R., Turlier, H., Nédélec, F., and Hiiragi, T. (2015). Pulsatile cell-autonomous contractility drives compaction in the mouse embryo. *Nature cell biology*, 17(7):849–855.

McKinney, W. (2010). Data structures for statistical computing in python. 56–61. In *Proc 9th Python Sci Conf (SCIPY 2010)*.

Meinhardt, H. (2006). Primary body axes of vertebrates: Generation of a near-cartesian coordinate system and the role of spemann-type organizer. *Developmental Dynamics*, 235(11):2907–2919.

Miyazaki, M., Chiba, M., Eguchi, H., Ohki, T., and Ishiwata, S. (2015). Cell-sized spherical confinement induces the spontaneous formation of contractile actomyosin rings in vitro. *Nature cell biology*, 17(4):480–489.

Mizuno, T., Yamaha, E., Kuroiwa, A., and Takeda, H. (1999). Removal of vegetal yolk causes dorsal deficencies and impairs dorsal-inducing ability of the yolk cell in zebrafish. *Mechanisms of development*, 81(1-2):51–63.

Mizuno, T., Yamaha, E., and Yamazaki, F. (1997). Localized axis determinant in the early cleavage embryo of the goldfish, carassius auratus. *Development Genes and Evolution*, 206:389–396.

Mohri, T. and Kyozuka, K. (2022). Starfish oocytes of a. pectinifera reveal marked differences in sperm-induced electrical and intracellular calcium changes during oocyte maturation and at fertilization. *Molecular Reproduction and Development*, 89(1):3–22.

Mönke, G., Sorgenfrei, F. A., Schmal, C., and Granada, A. E. (2020). Optimal time frequency analysis for biological data-pyboat. *BioRxiv*, pages 2020–04.

Newman, S. A. (2009). Ee just's "independent irritability" revisited: the activated egg as excitable soft matter. *Molecular Reproduction and Development: Incorporating Gamete Research*, 76(10):966–974.

Nojima, H., Rothhämel, S., Shimizu, T., Kim, C.-H., Yonemura, S., Marlow, F. L., and Hibi, M. (2010). Syntabulin, a motor protein linker, controls dorsal determination. *Development*, 137(6):923–933.

Ober, E. A. and Schulte-Merker, S. (1999). Signals from the yolk cell induce mesoderm, neuroectoderm, the trunk organizer, and the notochord in zebrafish. *Developmental biology*, 215(2):167–181.

Ota, K. G. and Abe, G. (2016). Goldfish morphology as a model for evolutionary developmental biology. *Wiley Interdisciplinary Reviews: Developmental Biology*, 5(3):272–295.

Özgüç, Ö., de Plater, L., Kapoor, V., Tortorelli, A. F., Clark, A. G., and Maître, J.-L. (2022). Cortical softening elicits zygotic contractility during mouse preimplantation development. *PLoS Biology*, 20(3):e3001593.

Pereyra, M., Drusko, A., Krämer, F., Strobl, F., Stelzer, E. H., and Matthäus, F. (2021). Quickpiv: Efficient 3d particle image velocimetry software applied to quantifying cellular migration during embryogenesis. *BMC bioinformatics*, 22:1–20.

Piccolo, S., Sasai, Y., Lu, B., and De Robertis, E. M. (1996). Dorsoventral patterning in xenopus: inhibition of ventral signals by direct binding of chordin to bmp-4. *Cell*, 86(4):589–598.

Postma, M. and Goedhart, J. (2019). Plotsofdata—a web app for visualizing data together with their summaries. *PLoS biology*, 17(3):e3000202.

Pourquié, O. (2011). Vertebrate segmentation: from cyclic gene networks to scoliosis. *Cell*, 145(5):650–663.

Rissi, M., Wittbrodt, J., Délot, E., Naegeli, M., and Rosa, F. M. (1995). Zebrafish radar: A new member of the tgf-β superfamily defines dorsal regions of the neural plate and the embryonic retina. *Mechanisms of development*, 49(3):223–234.

Roegiers, F., McDougall, A., and Sardet, C. (1995). The sperm entry point defines the orientation of the calcium-induced contraction wave that directs the first phase of cytoplasmic reorganization in the ascidian egg. *Development*, 121(10):3457–3466.

Salbreux, G., Joanny, J.-F., Prost, J., and Pullarkat, P. (2007). Shape oscillations of non-adhering fibroblast cells. *Physical biology*, 4(4):268.

Santella, L. and Chun, J. T. (2022). Structural actin dynamics during oocyte maturation and fertilization. *Biochemical and Biophysical Research Communications*, 633:13–16.

Sardet, C., Paix, A., Prodon, F., Dru, P., and Chenevert, J. (2007). From oocyte to 16-cell stage: cytoplasmic and cortical reorganizations that pattern the ascidian embryo. *Developmental Dynamics: An Official Publication of the American Association of Anatomists*, 236(7):1716–1731.

Sardet, C., Roegiers, F., Dumollard, R., Rouviere, C., and McDougall, A. (1998). Calcium waves and oscillations in eggs. *Biophysical chemistry*, 72(1-2):131–140.

Sasai, Y., Lu, B., Steinbeisser, H., Geissert, D., Gont, L. K., and De Robertis, E. M. (1994). Xenopus chordin: a novel dorsalizing factor activated by organizer-specific homeobox genes. *Cell*, 79(5):779–790.

Schindelin, J., Arganda-Carreras, I., Frise, E., Kaynig, V., Longair, M., Pietzsch, T., Preibisch, S., Rueden, C., Saalfeld, S., Schmid, B., et al. (2012). Fiji: an open-source platform for biological-image analysis. *Nature methods*, 9(7):676–682.

Sidi, S., Goutel, C., Peyriéras, N., and Rosa, F. M. (2003). Maternal induction of ventral fate by zebrafish radar. *Proceedings of the National Academy of Sciences*, 100(6):3315–3320.

Simon, J. Z. and Cooper, M. S. (1995). Calcium oscillations and calcium waves coordinate rhythmic contractile activity within the stellate cell layer of medaka fish embryos. *Journal of Experimental Zoology*, 273(2):118–129.

Spector, I., Shochet, N. R., Kashman, Y., and Groweiss, A. (1983). Latrunculins: novel marine toxins that disrupt microfilament organization in cultured cells. *Science*, 219(4584):493–495.

Straight, A. F., Cheung, A., Limouze, J., Chen, I., Westwood, N. J., Sellers, J. R., and Mitchison, T. J. (2003). Dissecting temporal and spatial control of cytokinesis with a myosin ii inhibitor. *Science*, 299(5613):1743–1747.

Stricker, S. A. (1999). Comparative biology of calcium signaling during fertilization and egg activation in animals. *Developmental biology*, 211(2):157–176.

Sun, Y.-H., Chen, S.-P., Wang, Y.-P., Hu, W., and Zhu, Z.-Y. (2005). Cytoplasmic impact on cross-genus cloned fish derived from transgenic common carp (cyprinus carpio) nuclei and goldfish (carassius auratus) enucleated eggs. *Biology of reproduction*, 72(3):510–515.

Tran, L. D., Hino, H., Quach, H., Lim, S., Shindo, A., Mimori-Kiyosue, Y., Mione, M., Ueno, N., Winkler, C., Hibi, M., et al. (2012). Dynamic microtubules at the vegetal cortex predict the embryonic axis in zebrafish. *Development*, 139(19):3644–3652.

Tsai, F.-C., Stuhrmann, B., and Koenderink, G. H. (2011). Encapsulation of active cytoskeletal protein networks in cell-sized liposomes. *Langmuir*, 27(16):10061–10071.

Tsai, H.-Y., Chang, M., Liu, S.-C., Abe, G., and Ota, K. G. (2013). Embryonic development of goldfish (carassius auratus): a model for the study of evolutionary change in developmental mechanisms by artificial selection. *Developmental dynamics*, 242(11):1262–1283.

Turing, A. M. (1952). The chemical basis of morphogenesis. *Bulletin of mathematical biology*, 52:153–197.

Uriu, K. (2016). Genetic oscillators in development. *Development, Growth & Differentiation*, 58(1):16–30.

Van Der Walt, S., Colbert, S. C., and Varoquaux, G. (2011). The numpy array: a structure for efficient numerical computation. *Computing in science & engineering*, 13(2):22–30.

Van der Walt, S., Schönberger, J. L., Nunez-Iglesias, J., Boulogne, F., Warner, J. D., Yager, N., Gouillart, E., and Yu, T. (2014). scikit-image: image processing in python. *PeerJ*, 2:e453.

Virtanen, P., Gommers, R., Oliphant, T. E., Haberland, M., Reddy, T., Cournapeau, D., Burovski, E., Peterson, P., Weckesser, W., Bright, J., et al. (2020). Scipy 1.0: fundamental algorithms for scientific computing in python. *Nature methods*, 17(3):261–272.

Waskom, M. L. (2021). Seaborn: statistical data visualization. *Journal of Open Source Software*, 6(60):3021.

Westfall, T. A., Hjertos, B., and Slusarski, D. C. (2003). Requirement for intracellular calcium modulation in zebrafish dorsal–ventral patterning. *Developmental biology*, 259(2):380–391.

Yamamoto, T.-o. (1934). On the rhythmic movements of the egg of goldfish. *J. Fac. Sci., Imp. Univ. Tokyo*, 3(3):275–285.

Yamamoto, T.-o. (1938). Contractile movement of the egg of a bony fish, salanx microdon. *Proceedings of the Imperial Academy*, 14(4):149–151.

Yamamoto, T.-o. (1954). Cortical changes in eggs of the goldfish (carassius auratus) and the pond smelt (hypomesus olidus) at the time of fertilization and activation. *Japanese Journal of Ichthyology*, 3(3-5):162–170.

Yu, P., Wang, Y., Li, Z., Jin, H., Li, L.-L., Han, X., Wang, Z.-W., Yang, X.-L., Li, X.-Y., Zhang, X.-J., et al. (2022). Causal gene identification and desirable trait recreation in goldfish. *Science China Life Sciences*, 65(12):2341–2353.

Supplementary Note 1: Supplementary Figures

Supplementary Figure F1: Goldfish embryos, unlike embryos of carp and of zebrafish, exhibit persistent rhythmic yolk contractions. (**A**) Detrended timeseries (via sinc-filter detrending, cut-off period = 850 seconds) of goldfish (GFxGF, magenta, n = 2), carp (CPxCP, blue, n = 2), and zebrafish (ZFxZF, green, n = 10) embryos at 6300–9290 seconds (or 01:45:00–02:34:50 hh:mm:ss) post-fertilization. (**B**) Temporal evolution of period at 6300–9290 seconds (or 01:45:00–02:34:50 hh:mm:ss) post-fertilization, obtained from wavelet analysis. The period evolution for each sample and the median of the periods are represented as a color-coded dashed line and a color-coded solid line, respectively. The color-coded shaded area corresponds to the interquartile range. These data are the same as those plotted in Figure 1E. (**C**) Temporal evolution of maximum wavelet power at 6300–9290 seconds (or 01:45:00–02:34:50 hh:mm:ss) post-fertilization, obtained from wavelet analysis. The evolution of wavelet power for each sample is represented here as a color-coded dashed line. A higher wavelet power (power > 3) means that a specified Morlet wavelet is more correlated to the signal than to white noise (Mönke et al., 2020).

Supplementary Figure F2: Rhythmic contractions persist even in yolk that is pinched off from dying embryos. (**A**) Snapshots (top row) and magnified images (bottom row) of yolk that is getting pinched off from a dying embryo over time (06:07:10–06:08:30 hh:mm:ss post-fertilization). Embryo was treated with 0.1 μg/mL nocodazole for $\sim$ 4 mins at $\sim$ 10 mins post-fertilization, and is the same embryo as the treated embryo (NOCO) illustrated in Figure 4A and shown in Supplementary Movie M6. Magenta arrowheads mark pinching off of the yolk. Scale bar = 500 μm. (**B**) Snapshots (top row) and magnified images (bottom row) of persistent contractions of yolk that is pinched off from a dying embryo (same sample as in panel A) over time (06:13:00–06:17:00 hh:mm:ss post-fertilization). Magenta symbols mark change in the shape of the pinched off yolk between consecutive snapshots. Scale bar = 500 μm. For more samples showing persistent contractions of yolk that is pinched off from a dying embryo, refer to Supplementary Movie M7.

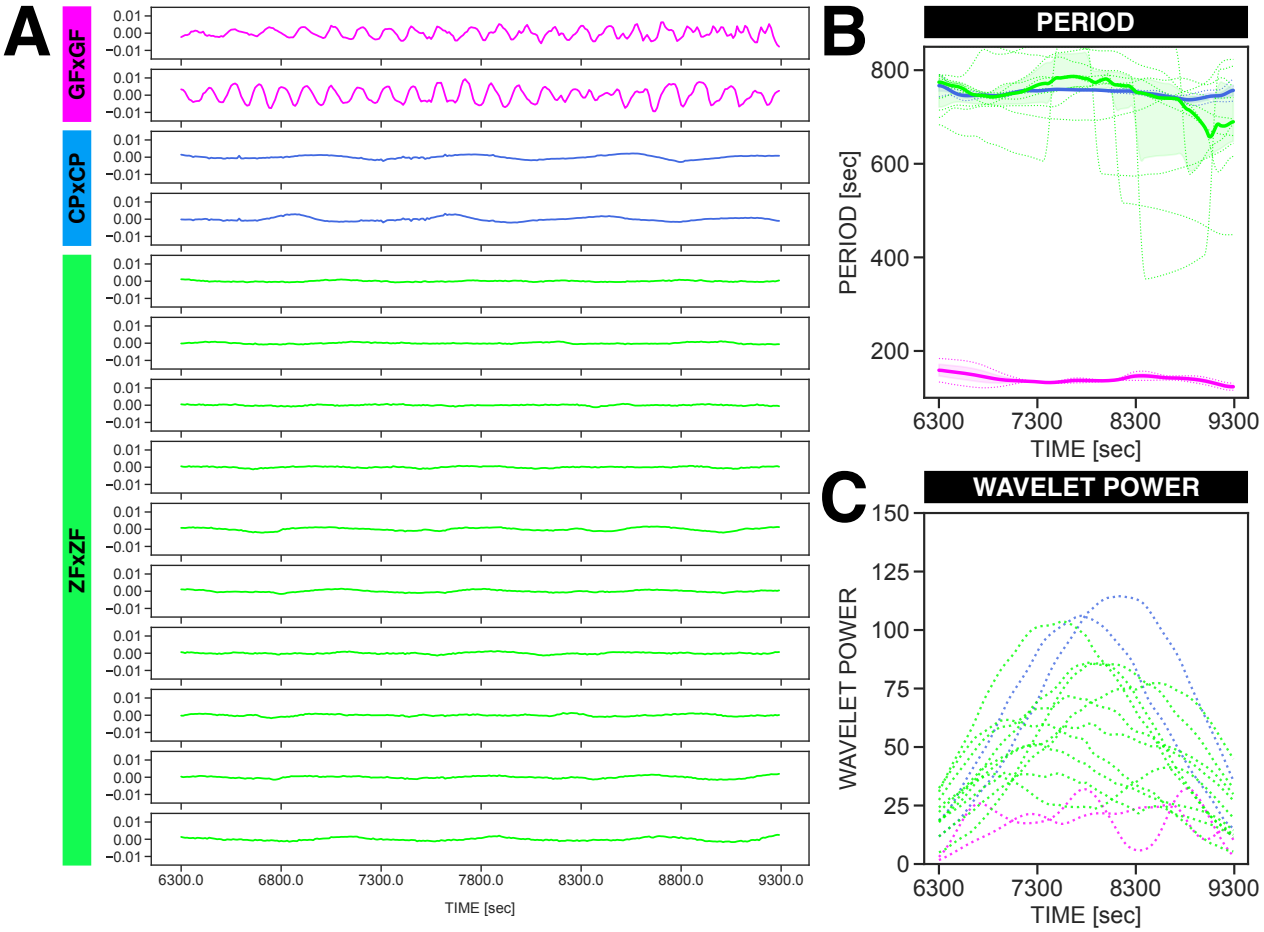

Fig. F1. Goldfish embryos, unlike embryos of carp and of zebrafish, exhibit persistent rhythmic yolk contractions. (**A**) Detrended timeseries (via sinc-filter detrending, cut-off period = 850 seconds) of goldfish (GFxGF, magenta, n = 2), carp (CPxCP, blue, n = 2), and zebrafish (ZFxZF, green, n = 10) embryos at 6300–9290 seconds (or 01:45:00–02:34:50 hh:mm:ss) post-fertilization. (**B**) Temporal evolution of period at 6300–9290 seconds (or 01:45:00–02:34:50 hh:mm:ss) post-fertilization, obtained from wavelet analysis. The period evolution for each sample and the median of the periods are represented as a color-coded dashed line and a color-coded solid line, respectively. The color-coded shaded area corresponds to the interquartile range. These data are the same as those plotted in Figure 1E. (**C**) Temporal evolution of maximum wavelet power at 6300–9290 seconds (or 01:45:00–02:34:50 hh:mm:ss) post-fertilization, obtained from wavelet analysis. The evolution of wavelet power for each sample is represented here as a color-coded dashed line. A higher wavelet power (power > 3) means that a specified Morlet wavelet is more correlated to the signal than to white noise (Mönke et al., 2020).

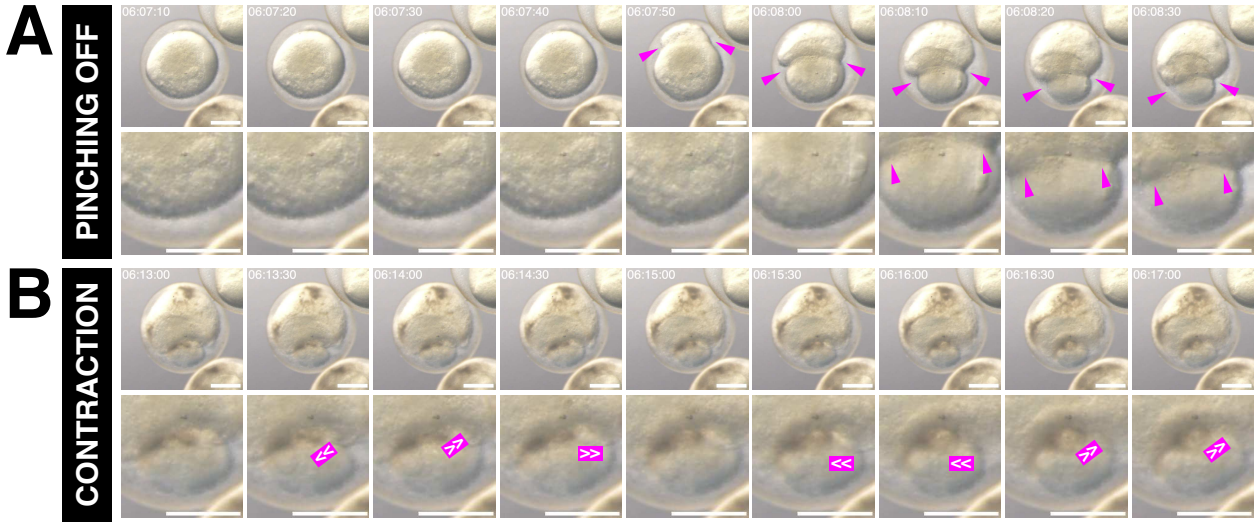

Fig. F2. Rhythmic contractions persist even in yolk that is pinched off from dying embryos. (**A**) Snapshots (top row) and magnified images (bottom row) of yolk that is getting pinched off from a dying embryo over time (06:07:10–06:08:30 hh:mm:ss post-fertilization). Embryo was treated with 0.1 μg/mL nocodazole for $\sim$ 4 mins at $\sim$ 10 mins post-fertilization, and is the same embryo as the treated embryo (NOCO) illustrated in Figure 4A and shown in Supplementary Movie M6. Magenta arrowheads mark pinching off of the yolk. Scale bar = 500 μm. (**B**) Snapshots (top row) and magnified images (bottom row) of persistent contractions of yolk that is pinched off from a dying embryo (same sample as in panel A) over time (06:13:00–06:17:00 hh:mm:ss post-fertilization). Magenta symbols mark change in the shape of the pinched off yolk between consecutive snapshots. Scale bar = 500 μm. For more samples showing persistent contractions of yolk that is pinched off from a dying embryo, refer to Supplementary Movie M7.

Supplementary Note 2: Supplementary Movies

Supplementary Movie M1: Goldfish embryos exhibit rhythmic yolk contractions from the 4-cell stage to the gastrula (epiboly) stage. Timelapse of goldfish embryos at different stages of development: zygote to cleavage stage at 00:21:00–01:43:00 hh:mm:ss post-fertilization, cleavage to blastula stage at 01:45:00–02:34:50 hh:mm:ss post-fertilization, blastula stage at 03:13:00–04:17:40 hh:mm:ss post-fertilization and at 04:31:00–05:10:10 hh:mm:ss post-fertilization, and gastrula (epiboly) stage at 07:28:30–09:06:10 hh:mm:ss post-fertilization. Scale bar = 500 μm. Movie is available at https://youtu.be/eqfiCiTJAA0. See also our video on early embryonic development of goldfish available at https://youtu.be/TVMull5YEqw?si=KZL156DdtBzQzqKA.

Supplementary Movie M2: Extracting the mean pixel value of an embryo (as proxy of projected area of the yolk) over time allows quantification of yolk contractions. Timelapse of goldfish embryo and its segmented yolk with raw timeseries of yolk circularity, yolk perimeter, yolk projected area, and embryo mean pixel value. Scale bar = 500 μm. Embryo is the same as embryo at cleavage-blastula stage in Supplementary Movie M1. Movie is available at https://youtu.be/Ai3maqIPxqo.

Supplementary Movie M3: Persistent and rhythmic contractions of the yolk are present in goldfish but not in closely-related carp or zebrafish. Timelapse of embryos of goldfish, carp, and zebrafish at 01:45:00–02:34:50 hh:mm:ss post-fertilization. Scale bar = 500 μm. Goldfish embryo is the same as embryo at cleavage-blastula stage in Supplementary Movie M1. Movie is available at https://youtu.be/dz3BtJsMTTs.

Supplementary Movie M4: The rhythmic contraction of the yolk is a trait that is maternal in origin. Timelapse of embryos of GF x GF goldfish, CP x CP carp, and their hybrids: (1) CP x GF from carp sperm and goldfish egg and (2) GF x CP from goldfish sperm and carp egg. Scale bar = 500 μm. Movie is available at https://youtu.be/7_dwYM4-PMw.

Supplementary Movie M5: The rhythmic contractions of the goldfish yolk are independent from fertilization or cell division, and emerge at a precise time. Timelapse of fertilized and unfertilized goldfish eggs at different time periods: cleavage stage at 00:33:00–01:53:40 hh:mm:ss post-exposure of egg (and sperm, for fertilized sample) to water, cleavage-blastula stage at 01:45:00–02:00:40 hh:mm:ss post-exposure of egg (and sperm, for fertilized sample) to water, and gastrula stage at 07:58:00–08:03:20 hh:mm:ss post-exposure of egg (and sperm, for fertilized sample) to water. Labels for each time period are based on developmental staging of fertilized samples. Scale bar = 500 μm. Note emergence of rhythmic yolk contractions in both samples from around 01:30:00 hh:mm:ss post-exposure of egg (and sperm, for fertilized sample), when the fertilized sample is at 4-cell stage. Also note failure of unfertilized samples to undergo cell divisions. The fertilized sample at cleavage-blastula stage is the same as the goldfish embryo at cleavage-blastula stage in Supplementary Movie M1. The fertilized sample at gastrula stage is the same as the goldfish sample (GF x GF) in Supplementary Movie M4. Movie is available at https://youtu.be/BRXBi_ahNLw.

Supplementary Movie M6: The rhythmic contractions of the goldfish yolk do not depend on microtubule polymerization prior to the first cleavage. Timelapse of goldfish embryos treated with either 0.1 μg/mL nocodazole (a microtubule-depolymerizing drug) or DMSO (as control) for $\sim$ 4 mins at $\sim$ 10 mins post-fertilization. At around 06:00:00–06:40:00 hh:mm:ss post-fertilization, note persistent contractions of yolk pinched off from nocodazole-treated embryo. Scale bar = 500 μm. Movie is available at https://youtu.be/S9sagyMPJvU.

Supplementary Movie M7: The rhythmic contractions of the goldfish yolk persist even in yolk that is pinched off from dying embryos. Timelapse of goldfish embryos showing persistent contractions of yolk that is pinched off from embryo. Embryos were treated with 0.1 μg/mL nocodazole for $\sim$ 4 mins at $\sim$ 10 mins post-fertilization. White arrows mark samples showing persistent yolk contractions of pinched off yolk. Specified numbers are some timepoints when these contractions are visible. Scale bar = 500 μm. Movie is available at https://youtu.be/e1eAFjDMdR8.

Supplementary Movie M8: Nocodazole-treated goldfish embryos exhibit altered yolk contraction dynamics. Timelapse of goldfish embryos treated with either 0.1 μg/mL nocodazole (a microtubule-depolymerizing drug) or DMSO (as control) for $\sim$ 4 mins at $\sim$ 10 mins post-fertilization, with corresponding detrended timeseries (via sinc-filter detrending, cut-off period = 250 seconds). Scale bar = 500 μm. These samples are the same as those in Supplementary Movie M6. Also shown are average period and amplitude (at maximum wavelet power) of yolk contractions in control (n = 2) and treated (n = 5) goldfish embryos at 4500–14490 seconds (or 01:15:00–04:01:30 hh:mm:ss) post-fertilization. Samples are represented as color-coded dots, while the median is denoted as a solid black line. These data are the same as those plotted in Figure 4E-F. Movie is available at https://youtu.be/VeSkzfpOB8Q.

Supplementary Movie M9: Rhythmic contractions of the yolk in twin-tail goldfish embryos are faster than those

in wild-type. Timelapse of wild-type and twin-tail (i.e. *Oranda*) goldfish embryos, with corresponding detrended timeseries (via sinc-filter detrending, cut-off period = 250 seconds). Scale bar = 500 μm. Also shown are average period and amplitude (at maximum wavelet power) of yolk contractions in wild-type (WT, n = 2) and twin-tail (OR, n = 5) goldfish embryos at 6840–9290 seconds (or 01:54:00–02:34:50 hh:mm:ss) post-fertilization. Samples are represented as color-coded dots, while the median is denoted as a solid black line. These data are the same as those plotted in Figure 5C-D. Movie is available at https://youtu.be/iXt0CEV5ut0.

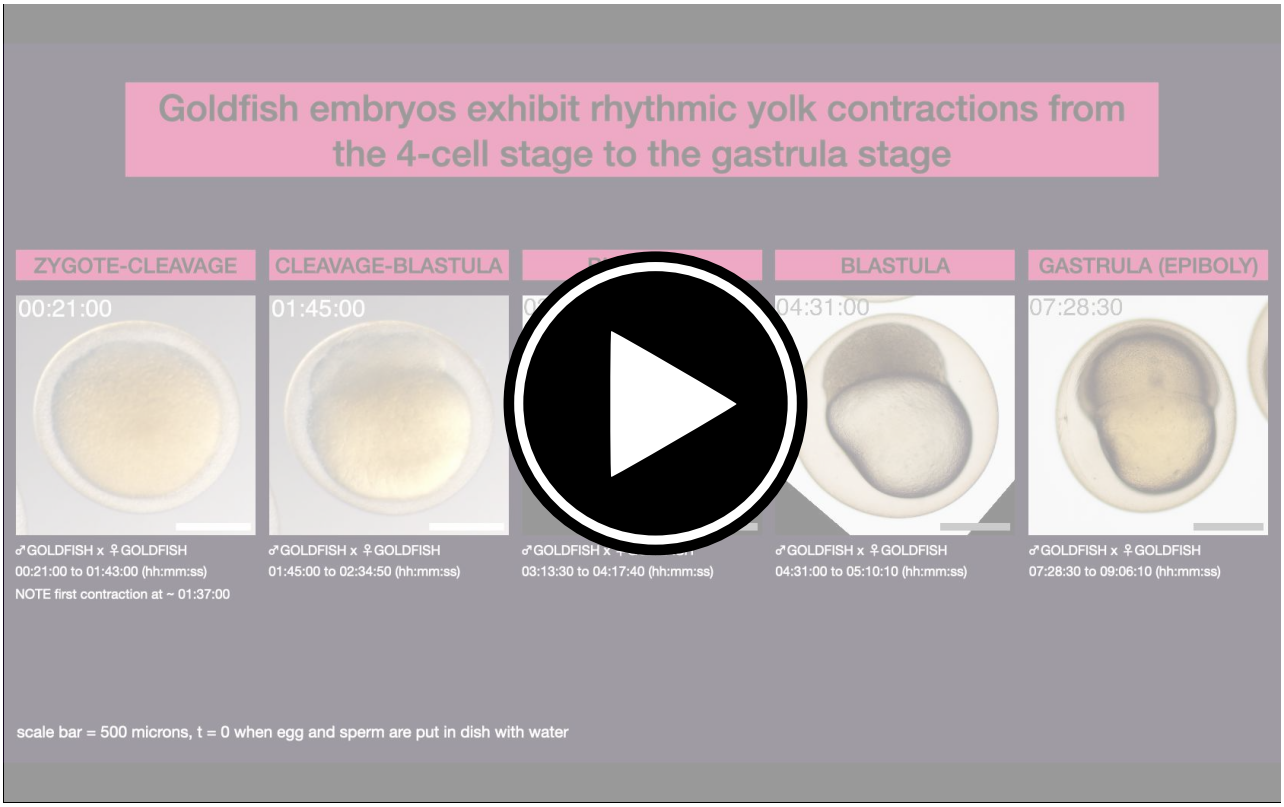

Fig. M1. Goldfish embryos exhibit rhythmic yolk contractions from the 4-cell stage to the gastrula (epiboly) stage. Timelapse of goldfish embryos at different stages of development: zygote to cleavage stage at 00:21:00–01:43:00 hh:mm:ss post-fertilization, cleavage to blastula stage at 01:45:00–02:34:50 hh:mm:ss post-fertilization, blastula stage at 03:13:00–04:17:40 hh:mm:ss post-fertilization and at 04:31:00–05:10:10 hh:mm:ss post-fertilization, and gastrula (epiboly) stage at 07:28:30–09:06:10 hh:mm:ss post-fertilization. Scale bar = 500 μm. Movie is available at https://youtu.be/eqfiCiTJAA0. See also our video on early embryonic development of goldfish available at https://youtu.be/TVMull5YEqw?si=KZL156DdtBzQzqKA.

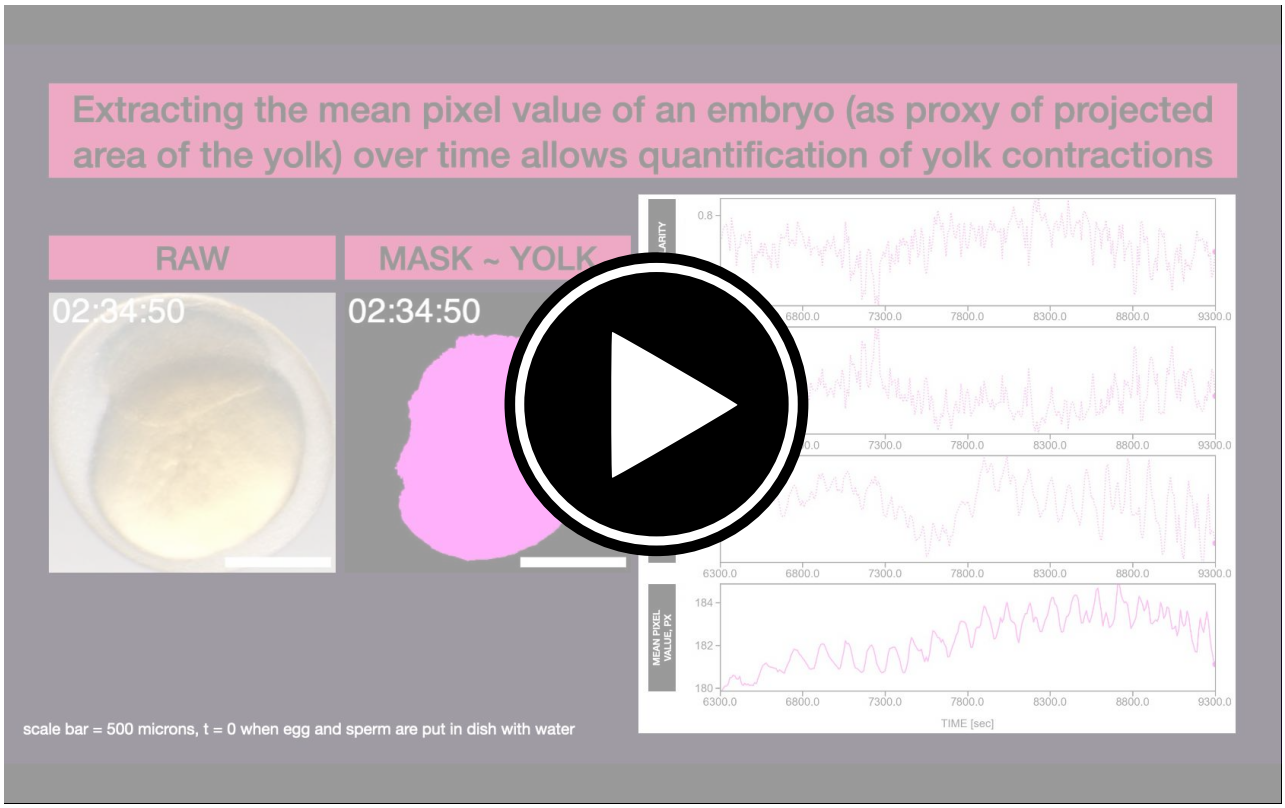

Fig. M2. Extracting the mean pixel value of an embryo (as proxy of projected area of the yolk) over time allows quantification of yolk contractions. Timelapse of goldfish embryo and its segmented yolk with raw timeseries of yolk circularity, yolk perimeter, yolk projected area, and embryo mean pixel value. Scale bar = 500 μm. Embryo is the same as embryo at cleavage-blastula stage in Supplementary Movie M1. Movie is available at https://youtu.be/Ai3maqIPxqo.

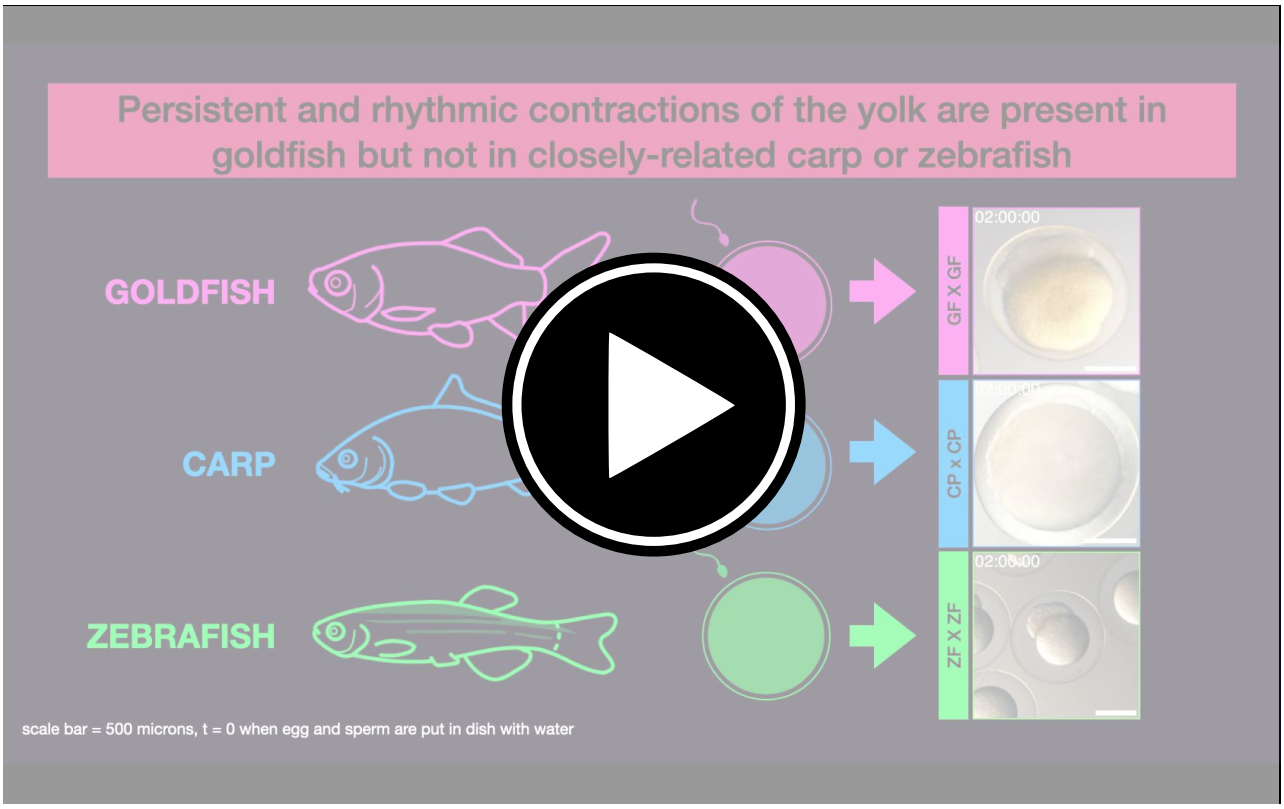

Fig. M3. Persistent and rhythmic contractions of the yolk are present in goldfish but not in closely-related carp or zebrafish. Timelapse of embryos of goldfish, carp, and zebrafish at 01:45:00–02:34:50 hh:mm:ss post-fertilization. Scale bar = 500 μm. Embryo is the same as embryo at cleavage-blastula stage in Supplementary Movie M1. Movie is available at https://youtu.be/dz3BtJsMTTs.

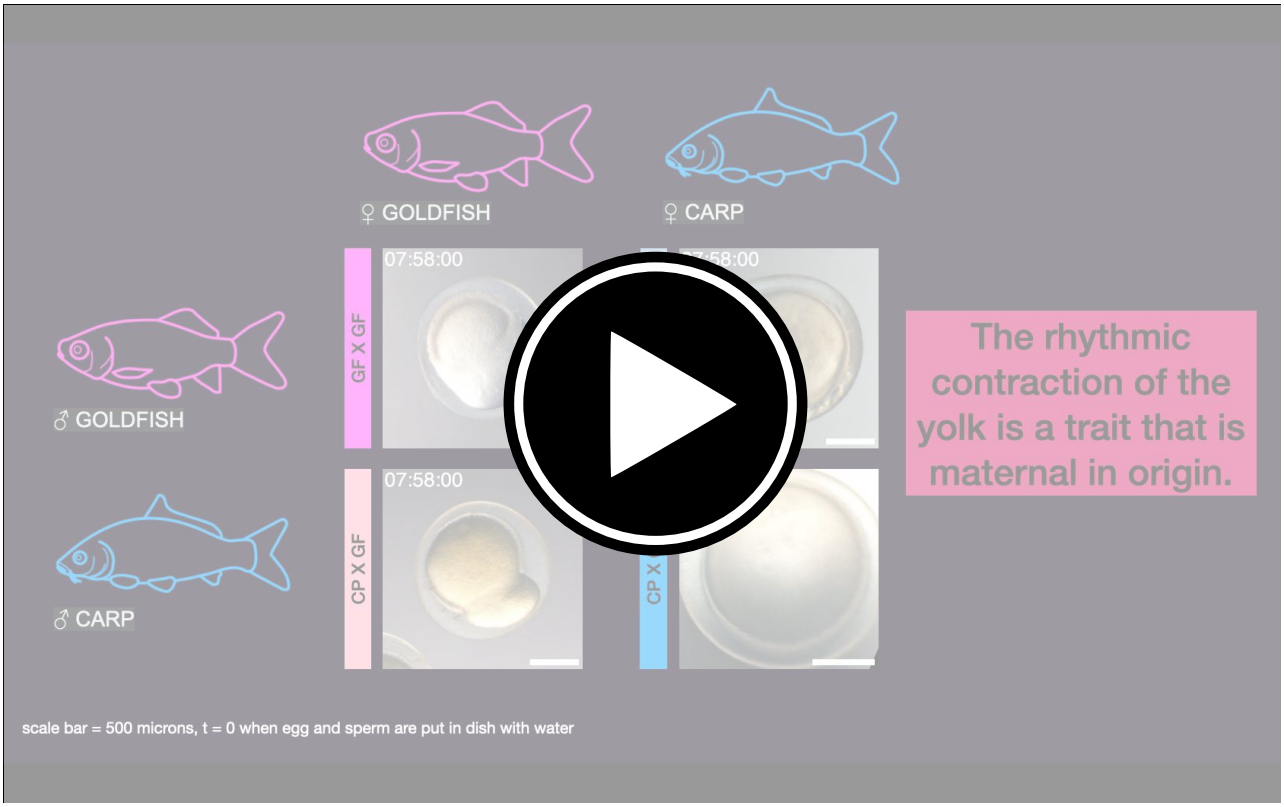

Fig. M4. The rhythmic contraction of the yolk is a trait that is maternal in origin. Timelapse of embryos of GF x GF goldfish, CP x CP carp, and their hybrids: (1) CP x GF from carp sperm and goldfish egg and (2) GF x CP from goldfish sperm and carp egg. Scale bar = 500 μm. Movie is available at https://youtu.be/7_dwYM4-PMw.

Fig. M5. The rhythmic contractions of the goldfish yolk are independent from fertilization or cell division, and emerge at a precise time. Timelapse of fertilized and unfertilized goldfish eggs at different time periods: cleavage stage at 00:33:00–01:53:40 hh:mm:ss post-exposure of egg (and sperm, for fertilized sample) to water, cleavage-blastula stage at 01:45:00–02:00:40 hh:mm:ss post-exposure of egg (and sperm, for fertilized sample) to water, and gastrula stage at 07:58:00–08:03:20 hh:mm:ss post-exposure of egg (and sperm, for fertilized sample) to water. Labels for each time period are based on developmental staging of fertilized samples. Scale bar = 500 μm. Note emergence of rhythmic yolk contractions in both samples from around 01:30:00 hh:mm:ss post-exposure of egg (and sperm, for fertilized sample), when the fertilized sample is at 4-cell stage. Also note failure of unfertilized samples to undergo cell divisions. The fertilized sample at cleavage-blastula stage is the same as the goldfish embryo at cleavage-blastula stage in Supplementary Movie M1. The fertilized sample at gastrula stage is the same as the goldfish sample (GF x GF) in Supplementary Movie M4. Movie is available at https://youtu.be/BRXBi_ahNLw.

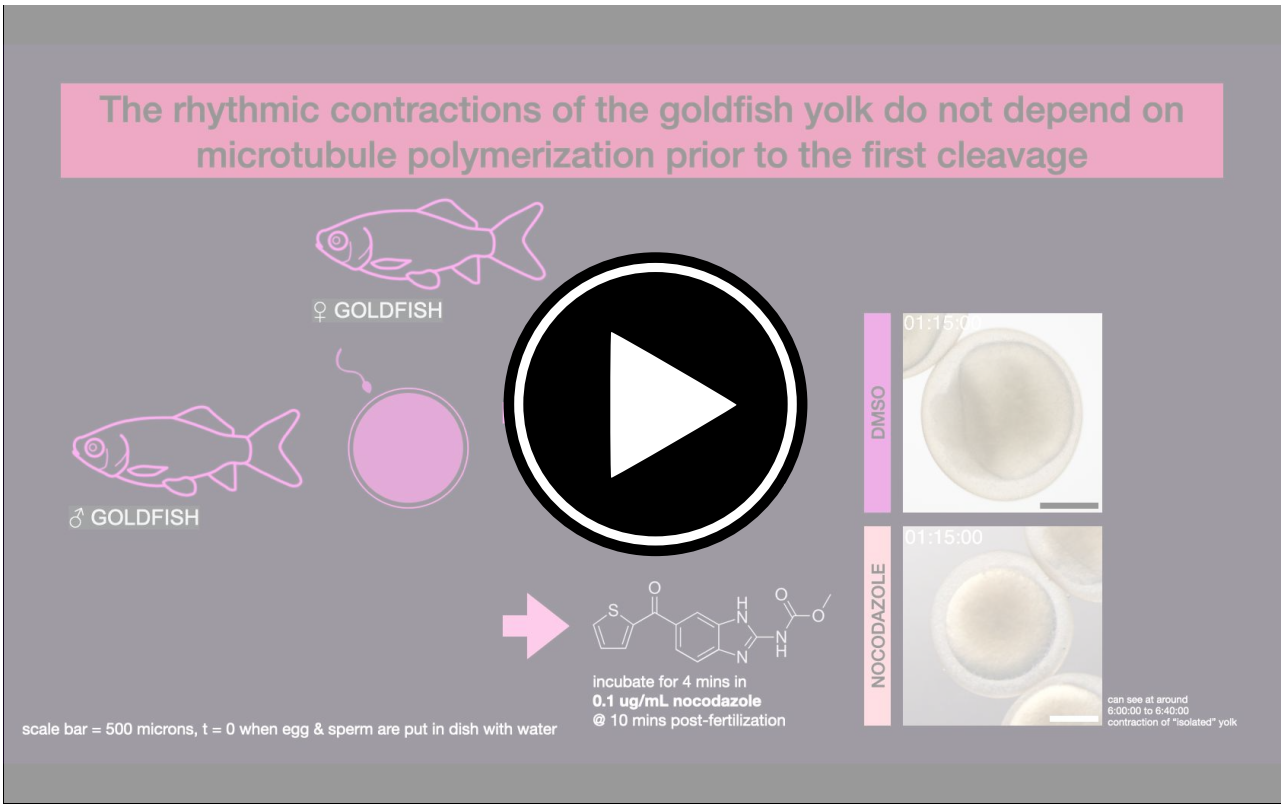

Fig. M6. The rhythmic contractions of the goldfish yolk do not depend on microtubule polymerization prior to the first cleavage. Timelapse of goldfish embryos treated with either 0.1 μg/mL nocodazole (a microtubule-depolymerizing drug) or DMSO (as control) for $\sim$ 4 mins at $\sim$ 10 mins post-fertilization. At around 06:00:00–06:40:00 hh:mm:ss post-fertilization, note persistent contractions of yolk pinched off from nocodazole-treated embryo. Scale bar = 500 μm. Movie is available at https://youtu.be/S9sagyMPJvU.

Fig. M7. The rhythmic contractions of the goldfish yolk persist even in yolk that is pinched off from dying embryos. Timelapse of goldfish embryos showing persistent contractions of yolk that is pinched off from embryo. Embryos were treated with 0.1 μg/mL nocodazole for $\sim$ 4 mins at $\sim$ 10 mins post-fertilization. White arrows mark samples showing persistent yolk contractions of pinched off yolk. Specified numbers are some timepoints when these contractions are visible. Scale bar = 500 μm. Movie is available at https://youtu.be/e1eAFjDMdR8.

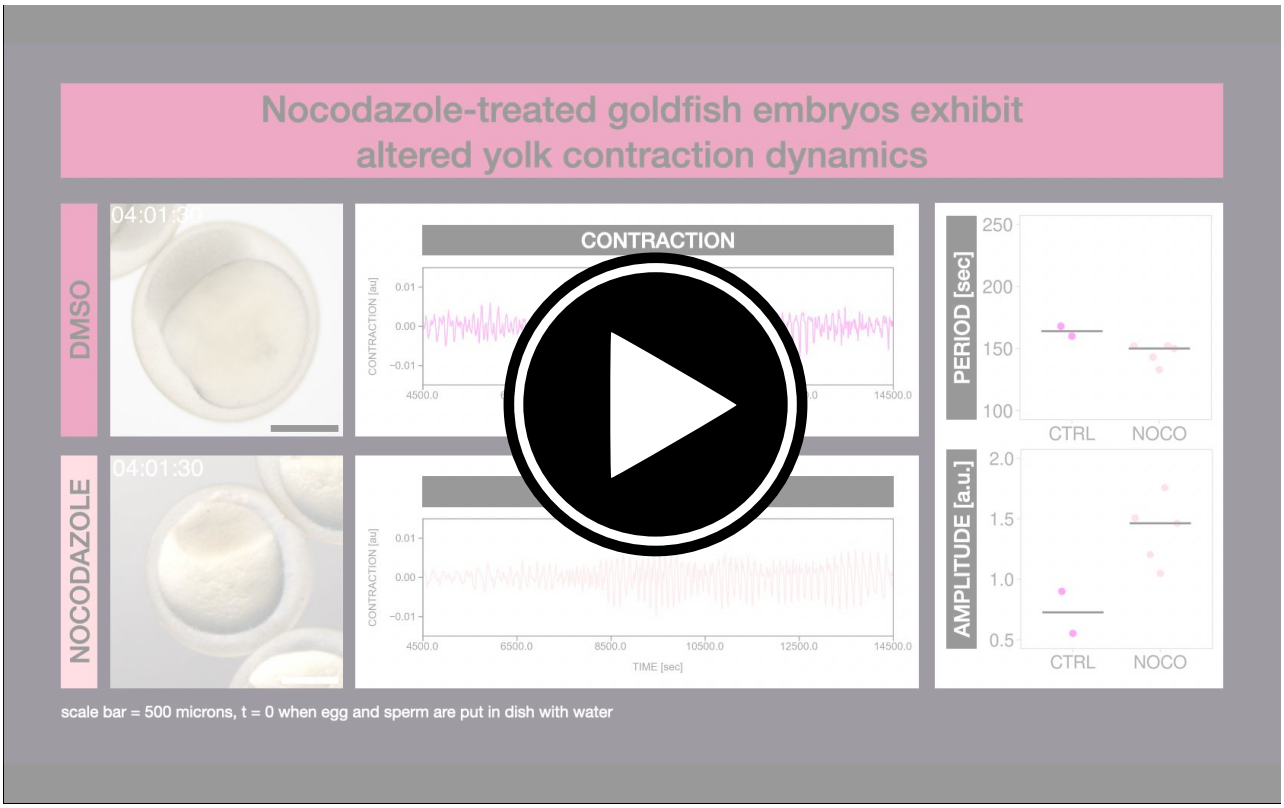

Fig. M8. Nocodazole-treated goldfish embryos exhibit altered yolk contraction dynamics. Timelapse of goldfish embryos treated with either 0.1 μg/mL nocodazole (a microtubule-depolymerizing drug) or DMSO (as control) for $\sim$ 4 mins at $\sim$ 10 mins post-fertilization, with corresponding detrended timeseries (via sinc-filter detrending, cut-off period = 250 seconds). Scale bar = 500 μm. These samples are the same as those in Supplementary Movie M6. Also shown are average period and amplitude (at maximum wavelet power) of yolk contractions in control (CTRL, n = 2) and treated (NOCO, n = 5) goldfish embryos at 4500–14490 seconds (or 01:15:00–04:01:30 hh:mm:ss) post-fertilization. Samples are represented as color-coded dots, while the median is denoted as a solid black line. These data are the same as those plotted in Figure 4E-F. Movie is available at https://youtu.be/VeSkzfpOB8Q.

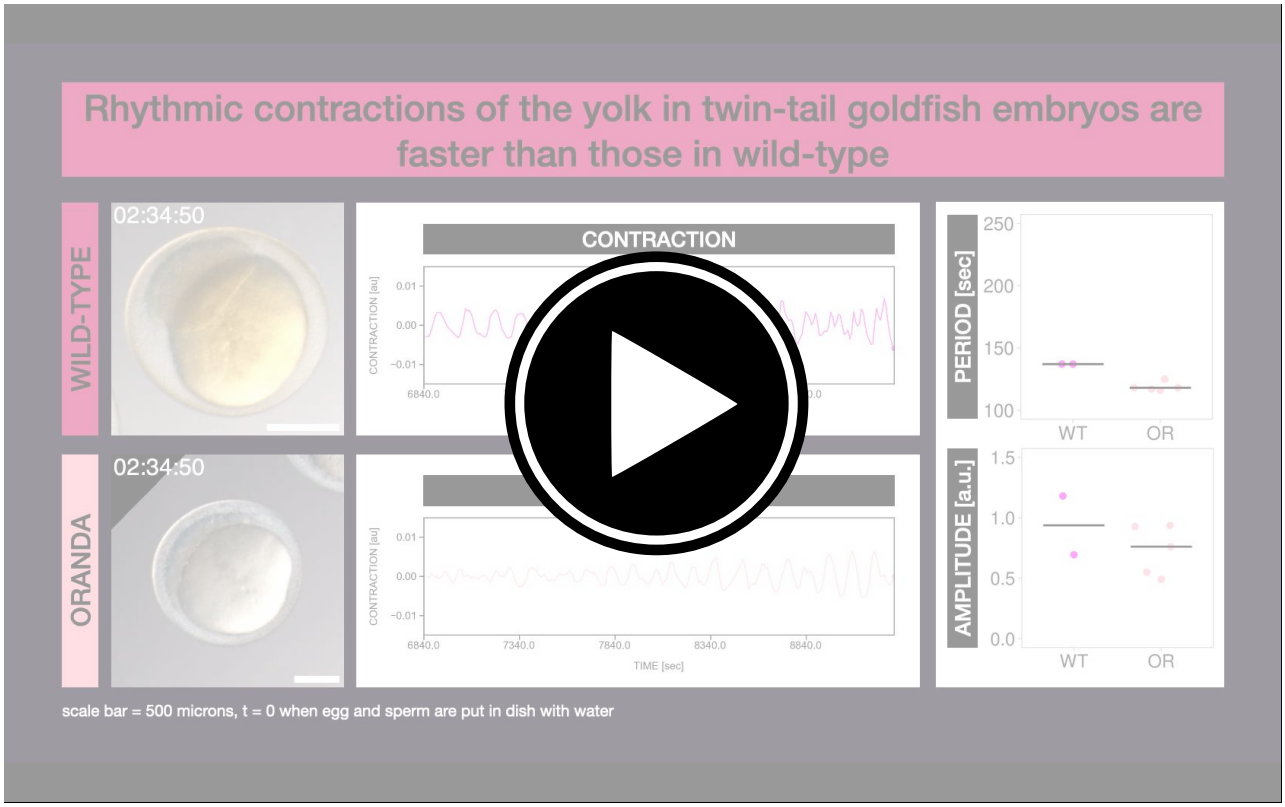

Fig. M9. Rhythmic contractions of the yolk in twin-tail goldfish embryos are faster than those in wild-type. Timelapse of wild-type and twin-tail (i.e. *Oranda*) goldfish embryos, with corresponding detrended timeseries (via sinc-filter detrending, cut-off period = 250 seconds). Scale bar = 500 μm. Also shown are average period and amplitude (at maximum wavelet power) of yolk contractions in wild-type (WT, n = 2) and twin-tail (OR, n = 5) goldfish embryos at 6840–9290 seconds (or 01:54:00–02:34:50 hh:mm:ss) post-fertilization. Samples are represented as color-coded dots, while the median is denoted as a solid black line. These data are the same as those plotted in Figure 5C-D. Movie is available at https://youtu.be/iXt0CEV5ut0.